FOILING SuMoth CHALLENGE

POLITO SAILING TEAM

Politecnico di Torino

Foiling SuMoth Challenge Stage 1 - 2024

DESIGN, MANUFACTURING & SUSTAINABILITY

sponsored by

11TH HOUR RACING

MARINESHIFT360

PERSICO

Bcomp®

TEAM NAME | UNIVERSITY NAME, CITY, COUNTRY | email@university.edu

Index

ABSTRACT

This report is about the design and manufacturing decisions behind VICTORIA, the latest addition to the Polito Sailing Team fleet. As the Kinks would sing, *VICTORIA is our queen*: the effort and determination we put into the concept reflect our devotion to the project and the entire team.
The experience gained from our oldest prototypes has given us the opportunity to reflect on the features we wanted in a boat. Thanks to the collaboration across all divisions of the team and our collective background, we succeeded in consolidating into a single prototype what was lacking in its predecessors.
VICTORIA has three main objectives, which are explored in detail throughout the report:

- **Performance**: while stability was the primary focus of the Sula project, this time we took a risk by aiming for speed. For this reason, the hull is narrower and lighter to ensure the greatest efficiency.
- **Modularity**: in the spirit of sustainability and continuous improvement, our aim was to construct a boat capable of serving the team for years to come. Every implemented part is designed to be adjustable and replaceable, allowing for a solid foundation (hull, deck, and internal structure) that can serve as a test bench for future team needs long after VICTORIA ceases competition.
- **Electronics**: the major challenge here was to develop an electronic control system that is fully reliable and capable of seamlessly transitioning from the mechanical system. Having tested it on SULA during training sessions, the results have been highly promising, and we look forward to implementing it on VICTORIA.

LIST OF TABLES

LIST OF FIGURES

1. ENGINEERING AND DESIGN

1.1. Preliminary design

For VICTORIA's preliminary design, we made use of the experience gained during the years with our previous prototypes.

Our first, KETH, was highly efficient from a hydrodynamic perspective but faced stability issues, making it challenging to handle on water. On the other hand, SULA was very stable but didn't meet our goals of volume, type, and performance.

Having established the maximum and minimum constraints for the new boat, and fixed certain variables such as displacement, stern, and bow shapes, we analyzed current market models: we paid particular attention to the Bieker V3 by Mackay, the Swift moth by Damic Design, and the Aerocet by Maguire. We analyzed the longitudinal waterlines of these designs to understand the targets needed to achieve the state-of-the-art.

1.2. Hull design

To achieve our goal of designing an optimized hull in terms of its hydrodynamic resistance, we chose to adopt an optimization software that employs the Response Surface Method: it generates an experimental design where the shape of the hull is enhanced to produce the least drag at take-off speed, making it easier to start the flight regime even in suboptimal wind conditions.
We began by outlining a preliminary hull and then applied various parameters to it so that it could be deformed in multiple ways. We then obtained the parameters values matching the hull design with the least drag through the Modefrontier optimization software.

1.2.1 Starting model

To outline the preliminary design, we focused on two types of moth hulls that are among the most common ones on the market: the Bieker and the Aerocet. The intention was to create a hull with parameters that would allow flexibility in its design, resembling the Bieker in some aspects and the Aerocet in others, depending on the values applied. Whilst this level of versatility was somewhat achievable, we felt it was more viable to start with a Bieker-type hull rather than trying to get close to the Aerocet design. This decision was driven by the compatibility of the Bieker model with our parameterization process.

1.2.2 Maxsurf

Using *Maxsurf Modeler*, we were able to outline a starting surface: to facilitate both parameterization and optimization, the starting surface itself had to be an acceptable design. This ensured that optimization didn't require extensive shape changes to the hull, as the parameters would naturally converge around established "standard" values, allowing for smoother processes. In developing the design, we considered several key factors: firstly, we ensured that the submerged volume would properly support both the weight of the boat (which we conservatively estimated at 50kg) and the weight of the sailor (85kg), then we fixed the waterline at least 15cm below the deck to promote stability. We also estimated the position of the center of gravity to anticipate the boat's trim once in the water; this estimate was based on observing professional sailors in the international Moth class and their position and movements during flight, in particular how far forward they were from the stern at take-off. Then, using *Maxsurf Stability*, we calculated the trim of the hull, paying close attention to the angle of heel and how much it varied by moving the center of gravity.

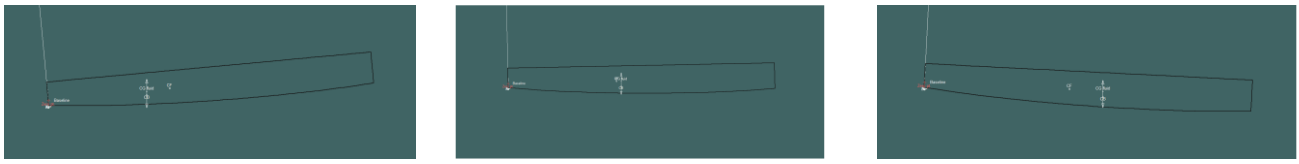

Figure 1-1: hull pitch at 3 different loadcase conditions

After several attempts we managed to define a satisfying design in terms of stability and displacement, so we passed it onto the next program for parameterization.

1.2.3 Caeses

The second software we adopted was CAESES 5, developed by Friendship System. CAESES is a powerful parametric 3D modelling and optimization tool, using advanced algorithms, including NSGA-II.

CAESES 5 enabled us to set up the project and begin to identify the desired modifications to the base hull. The software allows for each control point of the NURBS surface imported from Maxsurf to be associated with a specific value defined by a parameter. This value is added to the selected X, Y and Z coordinates to vary the position of the point in space and thus modify the hull design. Multiple parameters can be assigned to each point and the control point is positioned based on the sum of these parameters along with the initial position. Once the parameters and the desired variation for the hull are defined (for example, we assigned 7 parameters in one test), we proceed to the optimization phase. The software incorporates algorithms that

generate different hull models without the need for manual creation by the user, allowing a faster and more efficient workflow. These algorithms generate a selected number of hulls according to the limits of each parameter.

To continue with the optimization process, we connected CAESES 5 to the STAR CCM+ fluid dynamics simulation program. This allowed us to introduce the "target parameter", which automatically evaluates which hull generated by the algorithm is the most suitable. The chosen target parameter was "*drag*" : after completing the simulations, we obtained several hull models, all with acceptable drag values and in compliance with the competition rules.
The first CAD model, created manually and inspired by a "Bieker" model, is very different from the result, which resembles the shape of a gamma "Aerocet".

The starting model:

Figure 1-2: perspective view of the starting hull

CAESES optimized model:

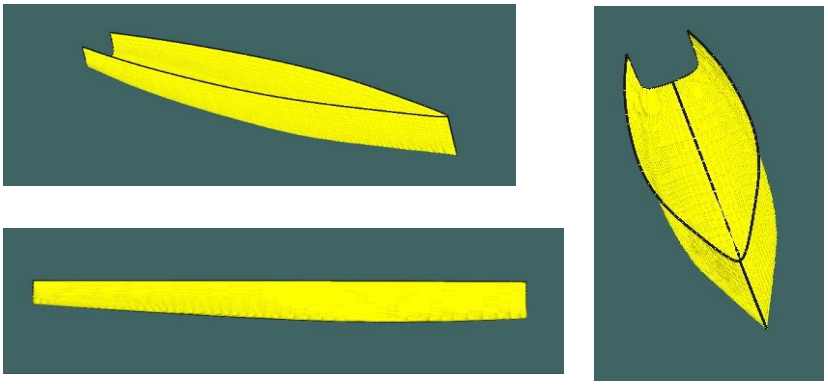

Figure 1-3: Perspective view of Caeses' optimized model

Despite the effectiveness of the program, we were not satisfied with the results and decided to use the knowledge gained to develop a better parameterized hull using Rhinoceros 3D modelling software and its integrated suites.

1.2.4 Grasshopper

Grasshopper is an extension to *Rhinoceros* that allows the software to be used in a way that is closer to block programming. This feature proved invaluable to us, as it enabled the use of sliders that *Modefrontier* (which we will discuss later) could automatically use as input parameters to modify geometry without external intervention. We used Grasshopper's "*control point deformation*" feature to ensure symmetrical adjustments to the hull, applying changes to only one half of the hull and then mirroring them around the central plane. The hull has 9 sections, each containing 7 control points. To limit the complexity of the Design of Experiments (DOE) while maximizing *Modefrontier*'s exploration capabilities, we focused on simple geometric parameters such as the width and depth of the bow, stern and overall hull.

The parameters we used were 6:

- "*Stern*" controls the width of the stern of the boat:

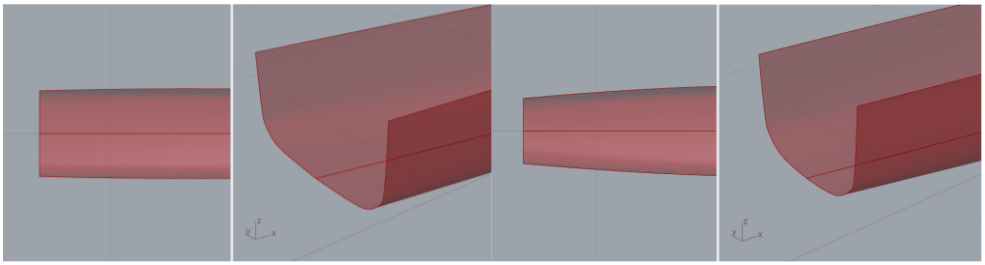

Figure 1-4: range of STERN parameter

- "*Depth*" controls the depth of the entire hull from stern to bow:

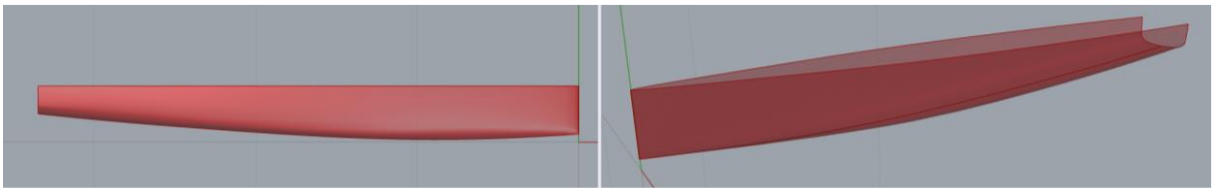

Figure 1-5: Range of DEPTH parameter

- "*Bow*" controls the width of the bow:

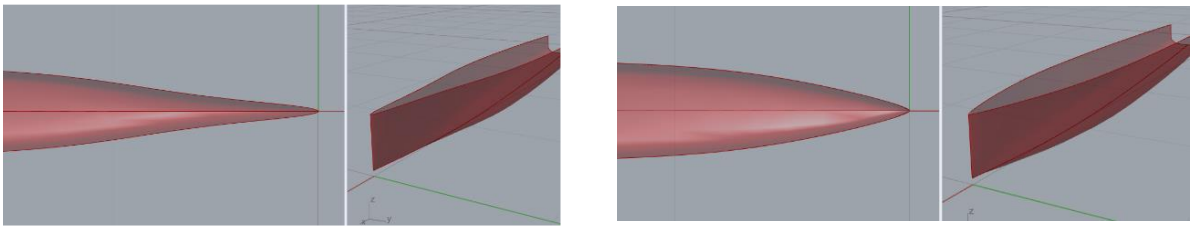

Figure 1-6: Range of BOW parameter

- "*Width*" controls the general width of the entire hull:

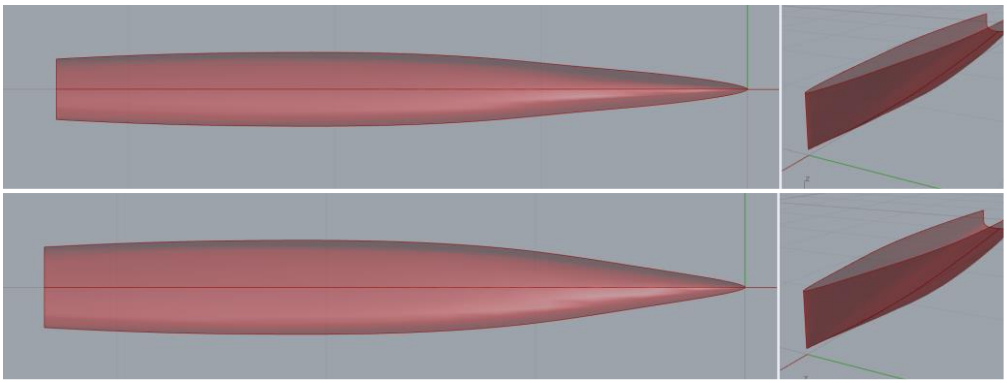

Figure 1-7: Range of WIDTH parameter

- "*Stern height*" is similar to depth but isolated on the stern:

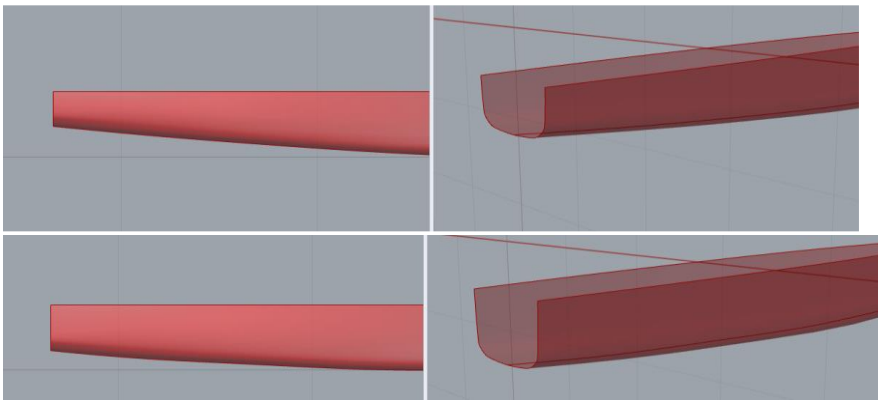

Figure 1-8: Range of STERN HEIGHT parameter

- "*Side*" controls the inclination of the sides:

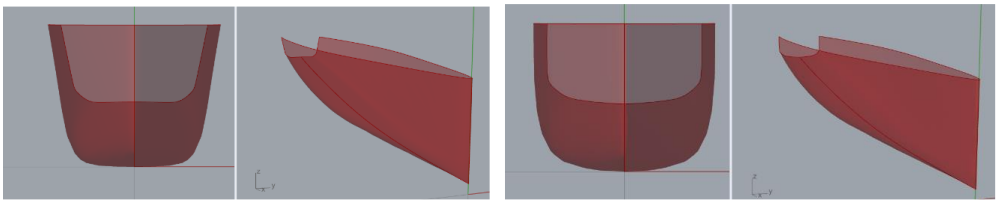

Figure 1-9: Range of SIDE parameter

After parametrization, we closed the hull by adding a temporary deck and stern, positioned so that the waterline was aligned with z=0 and the bow faced the origin of the x-axis. This revised hull model was then exported to IGES format to enable static simulations with *Star CCM*. We also used Grasshopper to ensure that the waterline of the hull after the modifications was at least 15cm below the deck, so that the volume

of the part of the hull below the set waterline limit was sufficient to keep the boat and sailors afloat, based on the weight estimates we had made earlier.

1.2.5 ModeFRONTIER

When we decided to change the software used to develop the models, we chose *ModeFRONTIER,* an optimization software developed by ESTECO.
The power of the software lies in its ability to generate a large number (10^4) of projects from a considerably smaller set of initial projects (10^2). It allows the creation of a Grasshopper-like workflow, built through the interaction of different "blocks", each with different functionalities. The workflow is described in the following figure, where the parameters used are listed in the top row, while the drag and volume target parameters appear below.

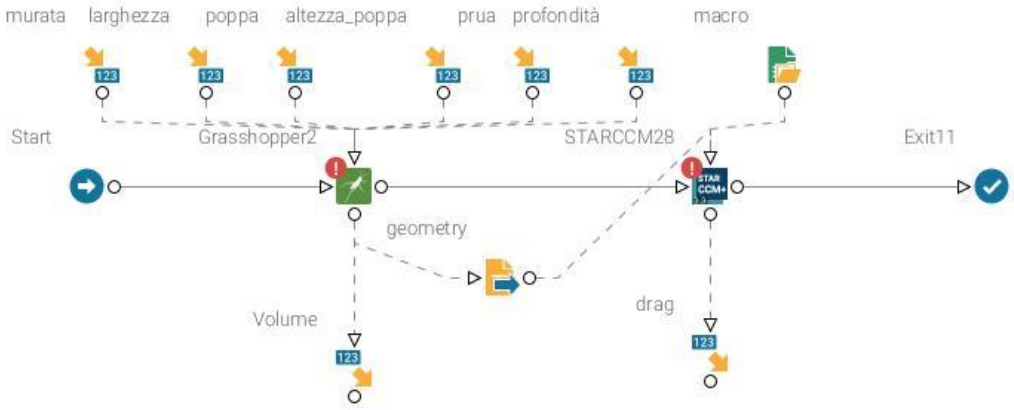

Figure 1-10: Modefrontier workflow

The software allowed us to use the ULH (Uniform Latin Hypercube) algorithm, which was designed to generate a DOE (Design of Experiment) suitable for the requirements of the RSM (Response Surface Method). ULH allowed the generation of a uniformly distributed array of designs in N-dimensional space, where N is the number of initial parameters. This approach provided insight into the dependence of results on specific combinations of parameters. The algorithm determined that 42 simulations (models) were required to gather the necessary information to generate the RSM.
Before starting the simulations, we imposed a constraint on the immersed volume to ensure buoyancy conditions under static conditions, which would provide a buoyancy force of approximately 1200N.
Finally, we started the simulation of the 42 initial projects, during which we encountered one error (due to a loss of network connection) and 2 unworkable projects (not complying with the set constraints).

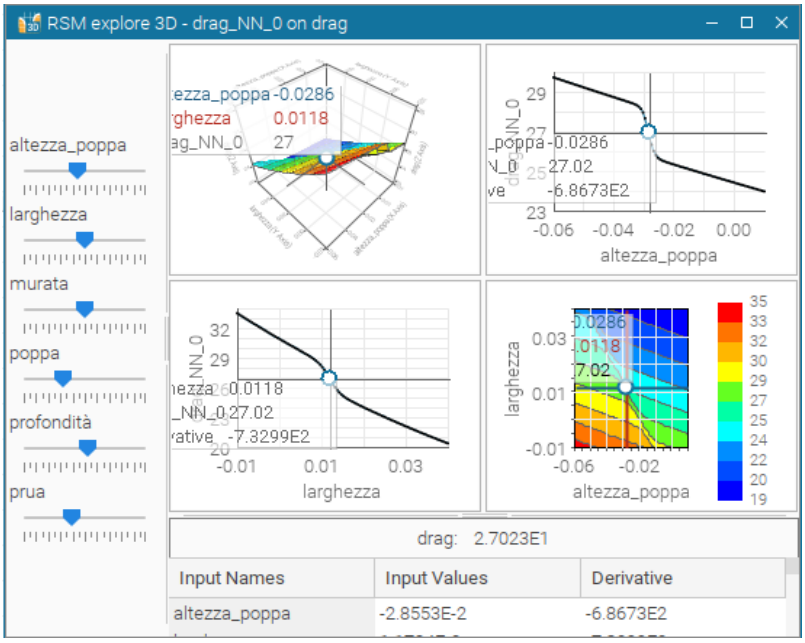

Figure 1-11:RSM graphs trained after the simulations

Then, thanks to a dedicated interface, we were able to develop an RSM based on a neural network that learned the relationships between the different parameters from the initial projects. Once the RSM was trained, we used it to generate 20,000 different designs using the PilOPT algorithm.

1.2.6 Star

We used Siemens STAR CCM+ software to simulate the hulls and assess the amount of drag they generate, but unfortunately, due to time and computing limitations, we could not run dynamic simulations for each project as we would have liked. Instead, we opted for static simulations carried out at a speed of 6 knots.
Using the expertise of our Computational Fluid Dynamics (CFD) team, we used a pre-defined template within the software.

Before starting the simulation, we used a Java script to make some necessary changes to the CAD models, as highlighted in the workflow. This script only facilitated these adjustments.

Once we had the results for the 42 projects foreseen by the DOE, we used the CFD software again to analyze some of the hulls produced. This step allowed us to validate the results through dynamic simulations with six degrees of freedom.

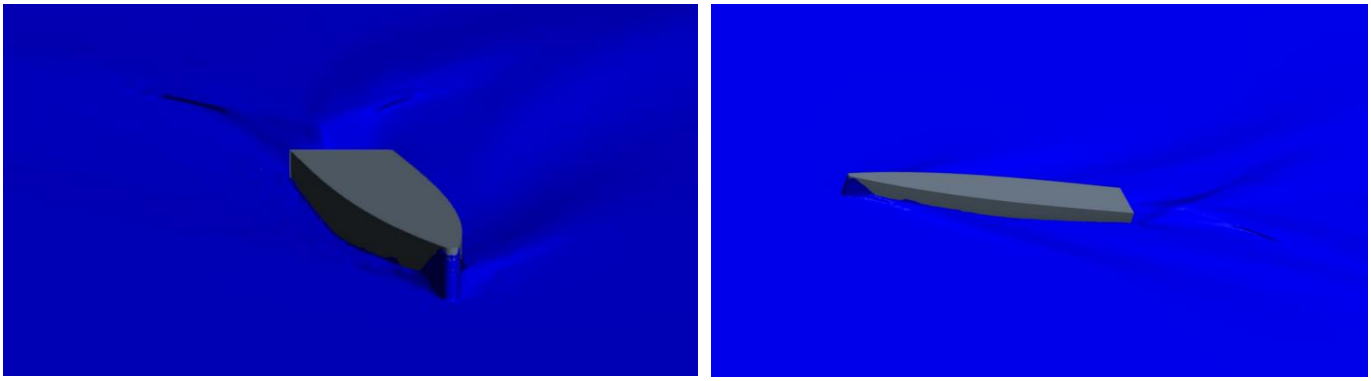

Figure 1-12: VOF of the final unsteady simulation

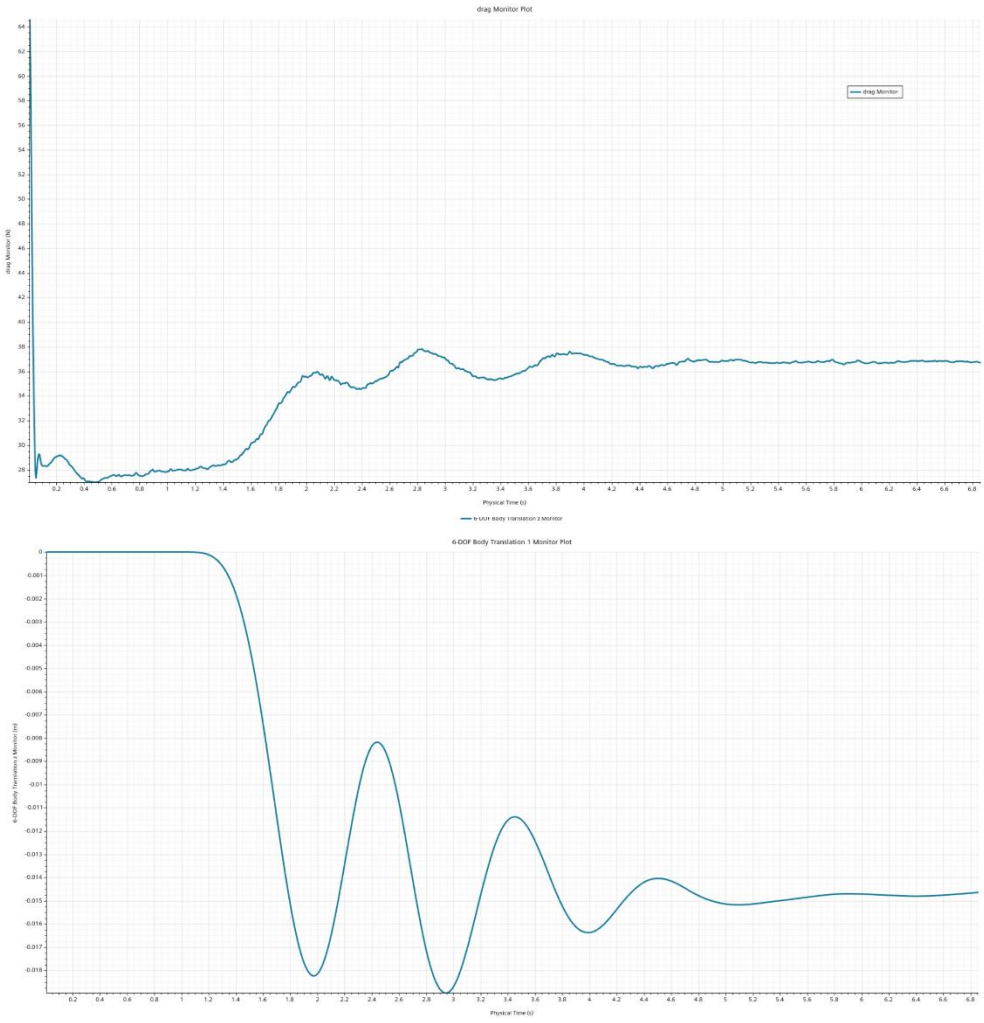

Figure 1-13: Star cm+ output graphs of z translation and drag

The results refer to half the hull.

The results were satisfactory and following some adjustments to the final CAD to correct anomalies, we transferred responsibility to the other areas involved in the project.

1.2.7 Conclusions

In the end thanks to *Modefrontier* we achieved a hull with remarkably low total drag at 3 m/s, and the resulting hull shape was overall valid.
However, we noticed that static simulations conducted without considering the real position of the LCB (Longitudinal Center of Buoyancy) tended to favor very slim bows, which is unusual as slim bows may cause negative trim angles, which means increased drag. Since our static simulations did not account for the LCB, these slim-bow hulls seemed to perform better. This uncertainty led us to try and take this whole workflow to another level, we put more effort and time into the bibliography to perfect both the optimization model and the parameterization of the hull. We also tried to find a more efficient way to measure the displacement of a parametric hull in Grasshopper without relying on external software, we performed static balance analyses for each hull, calculating the LCB and displacement to improve accuracy.

1.3. Deck and Wings

When designing the deck, we focused on the needs of the sailor and the rig. Our main objective was to create a piece where all the ropes, systems and other elements had a proper place to avoid clutter on the deck and prevent any obstructions that could inconvenience the sailor while sailing. We also optimized the design to have as flat a surface as possible to facilitate the manufacturing process..

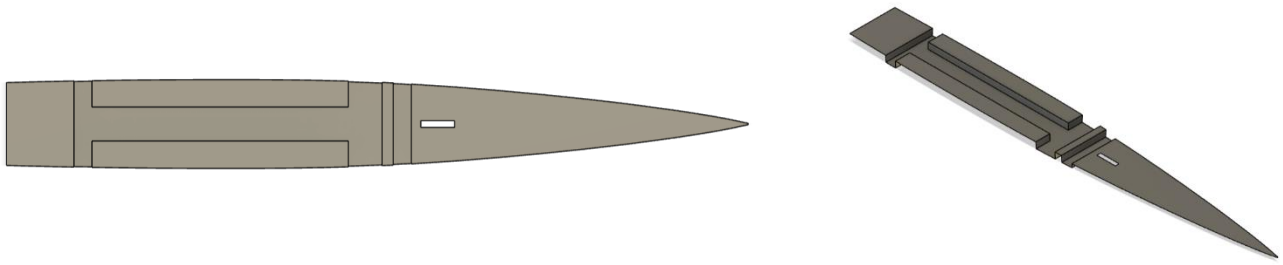

Figure 1-14: Deck design

We designed the deck with two transverse recesses at the stern and bow to accommodate the wings. In addition, a central recess intersects with another transverse recess to provide space for the circuitry needed to adjust the sail. The entire structure is covered by a panel, which was repurposed from a team-built component that was originally destined for disposal due to dimensional issues.

In designing VICTORIA's wings, we started by studying those built for SULA, paying close attention to construction issues and ergonomic factors related to the sailor's positioning while sailing. In terms of shape and positioning, we identified the need to increase the angle between the wing and the horizontal, as a less pronounced angle was uncomfortable for the sailor, especially during maneuvers.

In addition, although fabric wings can be cost effective, they wear out quickly and, if not properly tensioned, can increase drag as the sailor sinks into them. Over time, the method of attaching the cloth to the hull has also led to premature wear of the flange.
In response to these problems, and after studying the commercial solutions available, our design focused on the following points:

- Rigid wings
- Easy disassembly and transport
- Simplicity of manufacturing
- Marked curves to improve ergonomics and comfort.

One of our construction goals is to make the wings entirely of basalt. The structure includes several components: two symmetrical platforms (allowing them to be made from a single mold), two transverse pieces that close off the panels and fit into the deck recesses, and two upper profiles that secure the assembly.

To attach the shrouds to the structure, we will use *Ropeye* pass-through fittings with associated bushings and low friction rings. This will prevent the composite from being crushed, ensure even load distribution, and avoid point loads. We then install the sailor's harness attachments to ensure safety and comfort.

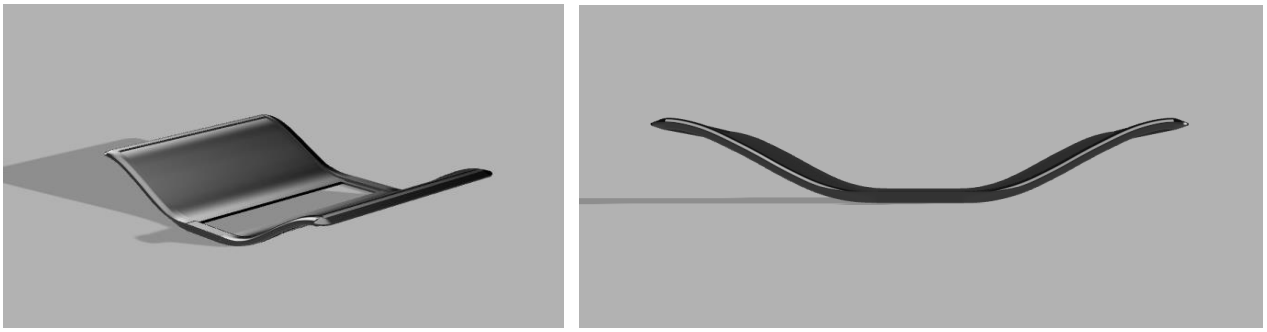

Figure 1-15: Wings design

1.4. Structural Analysis for hull, deck, and internal structure

The design of the internal structure is a crucial moment in the design process of a boat; it serves as a framework that provides rigidity and support to the hull and deck, which are subjected to significant loads from the weight of the sailor, the tensions of the rig and the lifting of the foils. It is designed as follows:

- A front spar, from bow to under the mast to withstand the bending moment produced by the forestay tension.
- A spar from under the mast to the centerboard housing to further withstand the bending moment.
- Two inclined ribs under the mast.
- Two half width ribs to support the centerboard housing.
- Two ribs to counteract the moment acting on the wings.
- A back spar that connects the stern wing supporting rib to the transom.
- A beam under the deck to provide stiffness.

1.4.1 Structural model

We carried out a detailed structural analysis to replicate real-world conditions, analyzing two subcases:

- Displacement regime: where the sailor stands at the most critical point on the deck, and only this load is considered.
- Stable flight condition: with the sailor positioned on a wing to counterbalance the capsizing moment.

The magnitudes are obtained from estimates of rigging stresses, geometric considerations, and fluid-dynamic simulations. Additionally, a safety factor has been considered.

Load	Magnitude [N]	Point of application
Forestay tension	2500	Head deck
Sailor's weight	1600	Wings rigid RBE
Lift of the centerboard foil	1010	Centerboard rigid RBE
Lift of the rudder foil	700	Rudder rigid RBE
Mast compression	3000	Mast
Shrouds	1600	Wings rigid RBE
Vang	8500	Mast
Cunningham	4000	Mast
Main Sheet	2000	Deck

Table 1-1: load for stable flight conditions subcase

Composite materials were chosen for the hull and deck to achieve high rigidity while minimizing weight, and Okumé wood for the internal structure. The best alternative for

the hull has proved to be a sandwich with a 6 mm PET core and a TWILL mineral fiber, a similar approach was taken for the deck with an 8mm PET.
Sustainability considerations led to the reuse of leftover sandwich material from previous projects, which was incorporated into the bow section of the deck. In addition to the base sandwich, reinforcement layers were strategically added in areas that we had identified through simulation as being most stressed.

Material	Mechanical properties	Magnitude
UD Basalt fiber	E_1	36115 [MPa]
	E_2	8713 [MPa]
	ν_{12}	0.322
TWILL Basalt fiber	E_1	31449 [MPa]
	E_2	31449 [MPa]
	ν_{12}	0.15
PET	E_1	112 [MPa]
	ν	0.3
Okoumè	E	7800 [MPa]
	ν	0.02

Table 1-2: hull, deck, internal structure materials

The simulations we ran showed that the most stressed areas were:

- The deck during the displacement regime
- The area of the wings, the attachment points of the bowsprit and the mast foot, during stable flight conditions

However, the displacement observed is minimal compared to the boat's size, and the stresses remain below the yield point.

To further reduce the weight of the boat, we carried out a topological optimization of the internal structure: by interpreting the results of the FEM analysis, we were able to choose a geometry that ensured acceptable rigidity and low weight.

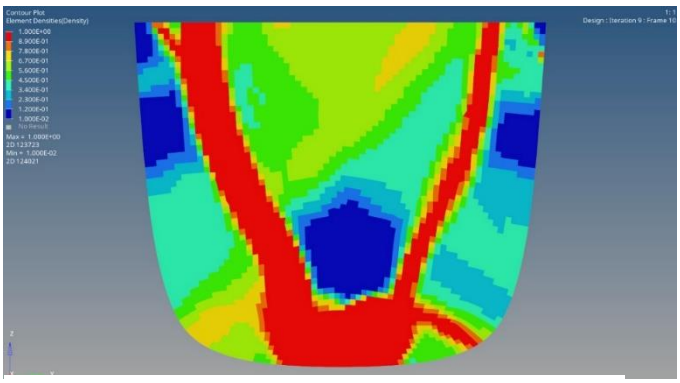

Figure 1-17: results of the FEM analysis of the most loaded rib

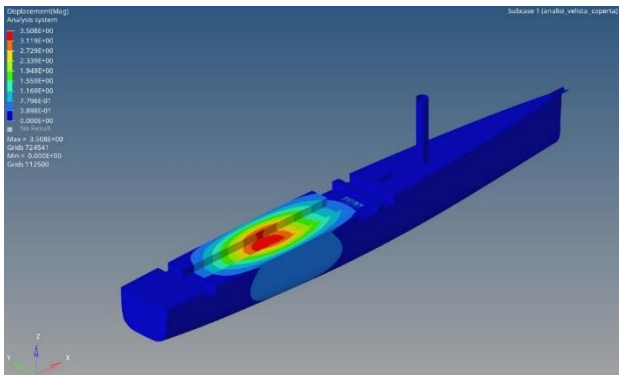

Figure 1-16: displacement of the hull and deck (subcase 1)

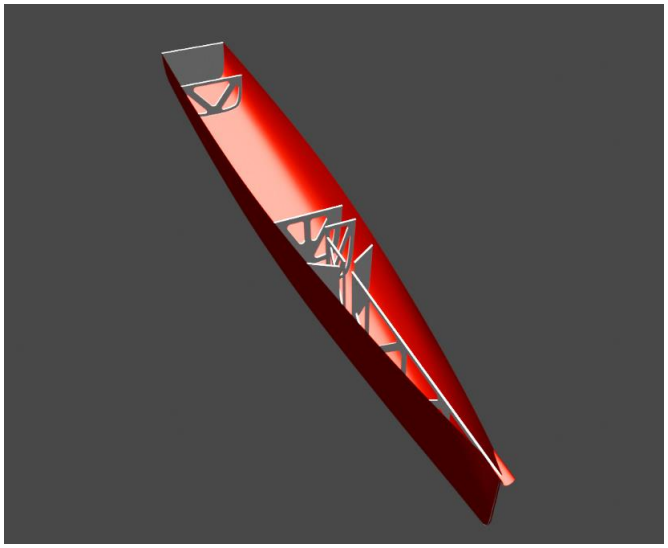

Figure 1-18: Internal Structure

1.5. Foils

The design process began with an analysis of the main shortcomings of SULA. Taking into account feedback from our sailors and analysis of the boat's architecture, we agreed that the main problem was the large size of the lifting surfaces, which allowed for easy launching and high stability, but severely limited top speed.

1.5.1 Airfoil selection

The first step in the design was to select an airfoil. For SULA we used the NACA 63-412 profile. However, extensive research led us to prefer the Eppler 393 profile for VICTORIA. This profile offers a superior lift-to-drag ratio at various angles of attack and has no worse stall behavior, making it ideal for our application. Additionally, this geometry is less likely to cause problem during manufacturing.

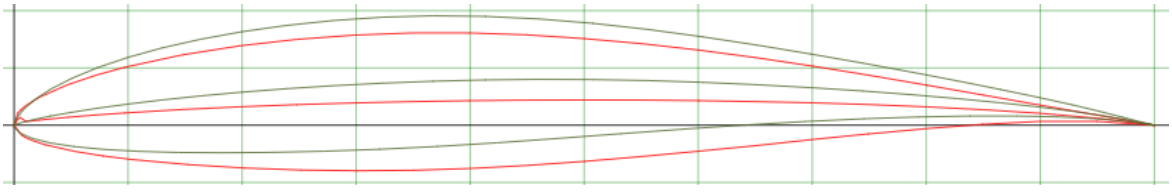

Figure 1-19: NACA 63-412 (red) vs EPPLER 393 (green)

The graph below shows the efficiency trend of the two profiles for a Reynolds of 500000: the purple curve represents NACA 63-412 and the yellow one Eppler 393's efficiency.

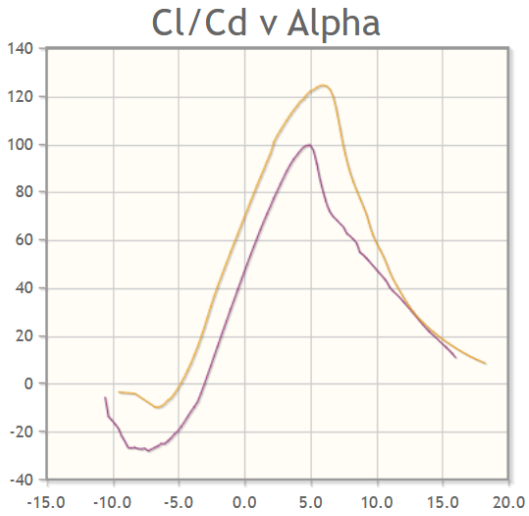

Figure 1-20: NACA 63-412 (purple) vs EPPLER 393 (yellow) efficiency

Thicker airfoils were chosen because they would allow easier accommodation of the connecting structures between the horizontal and vertical sections, as well as the insert for the flap control system. After comparing various options through CFD performance analysis, the Fage & Collins 3 airfoil was selected.

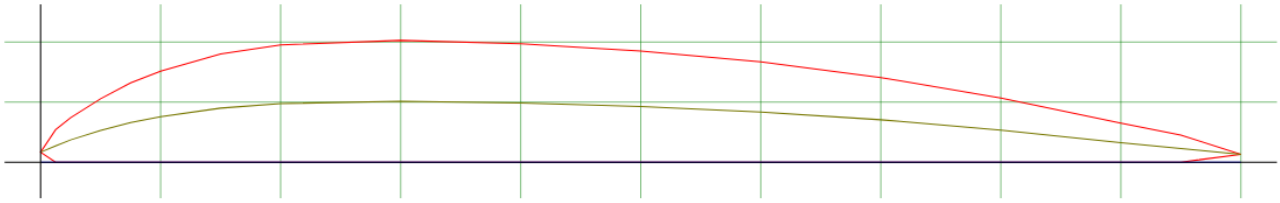

Figure 1-21: Fage & Collins 3 profile

1.5.2 Architecture

For the architectural design, we had to start with a preliminary estimate of the masses: we obtained them both by studying commercial examples and by relying on our past experience. The total mass should be around 125 kg, of which 45 kg for the hull and 80 kg for the sailor, so that the foils should generate a lift of 1225 N, a rather conservative approximation considering that the sail also exerts a certain lift force when the boat is rolled (decomposition of vector F_{sail} in $y_A - z_A$ axes).

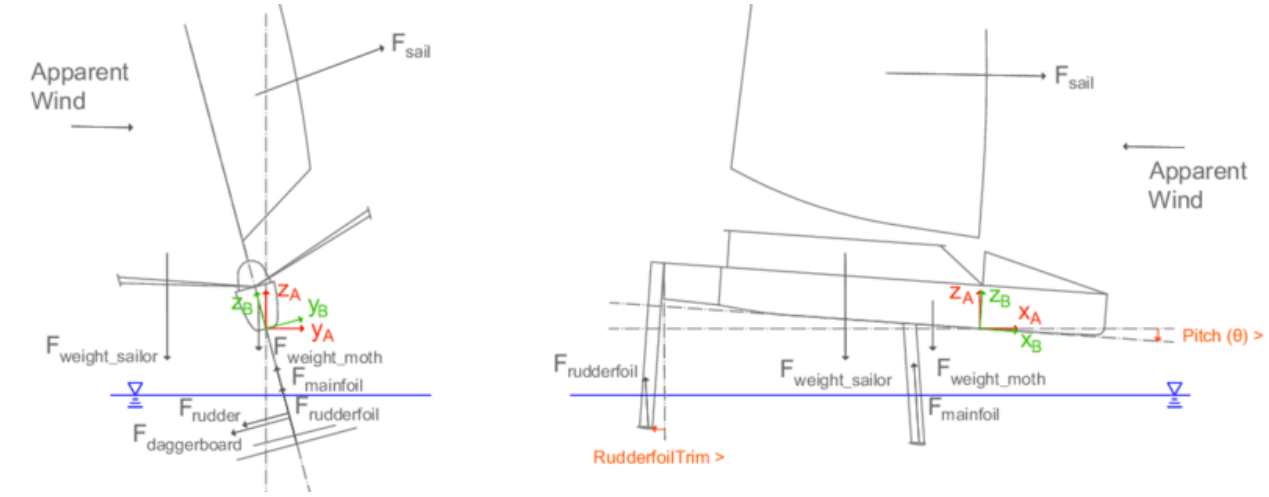

Figure 1-22: Forces diagrams

The maximum lift of the main foil was set at 70% of the total weight, with the remaining 30% supported by the rudder. With these assumptions, we estimated the hydrodynamic performance of the foils using panel method simulations with the *xflr5* software. After comparing different speed conditions and flap configurations, we found that a flap length of approximately 30% of the foil chord offered the best compromise between lift and efficiency. This analysis provided us with polar estimates for our lifting surfaces.

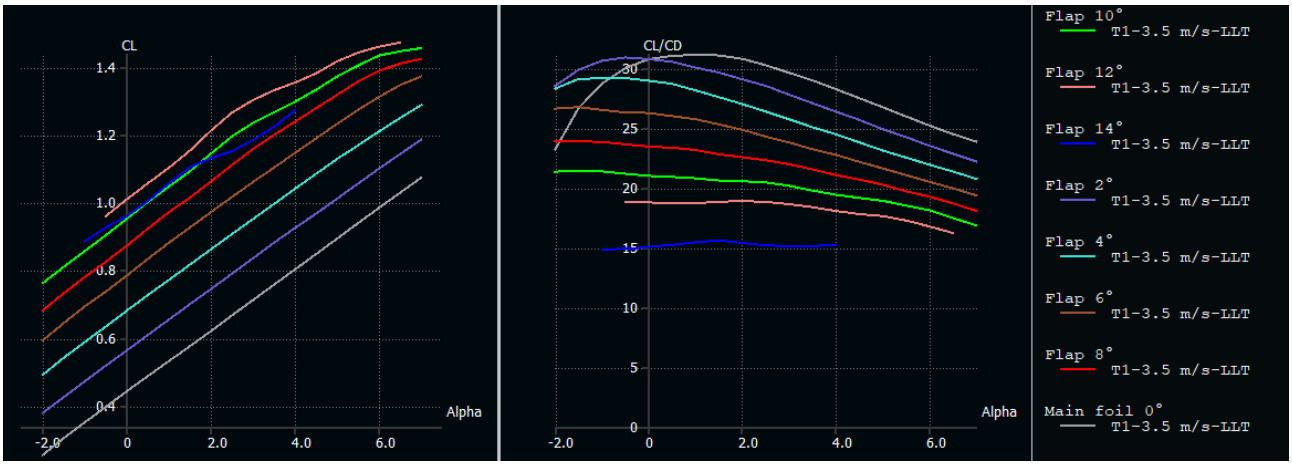

Figure 1-23: polars estimations with xflr5

This data was then used in an optimization tool developed by the team over the years in MATLAB to determine the optimal configuration of foil sizes and positions. This tool uses MATLAB's genetic algorithm capabilities to maximize efficiency across a range of sailing conditions while maintaining both static and dynamic stability. The algorithm takes the geometry of the boat as input and aims to find the equilibrium solution for the system at different speeds. The performance of this geometry is then evaluated by calculating the

drag coefficient C_D and the stability coefficient C_{M_α}. The purpose of the genetic algorithm is to minimize the objective function, which is the sum of the weighted performance parameters over the whole speed range:

$$objective\ function = \sum_{V_{min}}^{V_{max}} (K_1 \cdot C_D(i) + K_2 \cdot C_{M_\alpha})$$

Equation 1-1

The following assumptions have been made:

- The dimensions and hydrodynamic characteristics of the fixed vertical appendages are assumed to be the same as those of SULA.
- Sail performances are fixed, and come from the experimental data of Boegle's thesis[1].
- Speed ranges from 3.5 m/s to 11.5 m/s with 1 m/s increment.
- The maximum lift of the main foil is set to 70% of the system weight.
- Aspect ratios for the main and control surfaces are set to 11 and 9 respectively. These values have been determined in consultation with the Structures Division to ensure that wing deflection in flight remains at an acceptable level.
- The center of pressure position of the rudder along the longitudinal axis is set to the highest possible value as this improves stability.

After evaluating different trials of the tool with a maximum number of iterations of 100 and a maximum population size of 200 for the genetic algorithm, we obtained the final configuration:

S_{MF}	$\alpha_{set\ MF}$	x_{MF}	S_{RF}	x_{RF}
0.11 m^2	2°	1.4 m	0.06 m^2	3.835 m

Table 1-3: final configuration (MF – main foil, RF – rudder foil, distances from the bow)

1.5.3 Fluid dynamics optimization

To optimize the fluid dynamics of the foils we employed *Modefrontier* from ESTECO.

A parametric CAD model was first created using SolidWorks. The model was designed so that the lift area and aspect ratio could be defined as input parameters, ensuring that they remained constant with any changes to the wing shape. The leading and trailing edges were defined by Bezier curves, each with four control points.

[1] Evaluation of the Performance of a Hydro-Foiled Moth by Stability and Force Balance Criteria, C. Bögle, 31. Symposium Yachtbau und Yachtenwurf Hamburg, November 2010

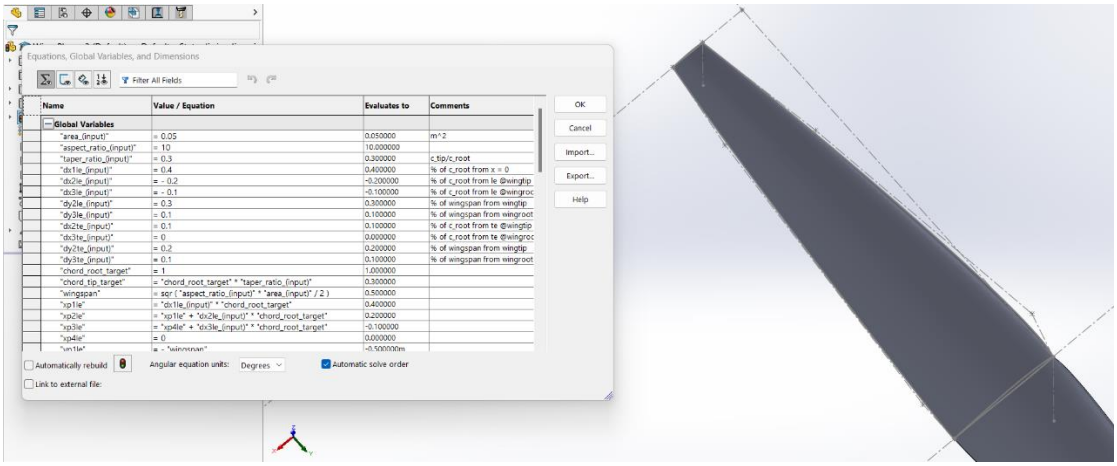

Figure 1-24: Parametric CAD of the foil

This approach allowed a wide range of designs to be explored, but would have required a long optimization process. We therefore decided to focus the design on near-elliptical shapes, which are known for their exceptional efficiency. This reduced the number of free parameters to optimize to four.
Modefrontier was used to generate a response surface, a statistical model based on performance calculations for a subset of designs, and ultimately to identify the optimal solution.

A suitable Design Of Experiment (DOE) was generated using the Uniform Latin Hypercube algorithm, containing 32 designs. Their efficiency was then assessed by CFD analysis using Siemens' *Star CCM+* software. The simulations were designed to capture the performance at high speed (8 m/s), with the foils set at an incidence of 0°.
The results of these sample cases were then used to train the response surface using the Modefrontier neural network. The PILOPT algorithm was then used to identify the optimal design.

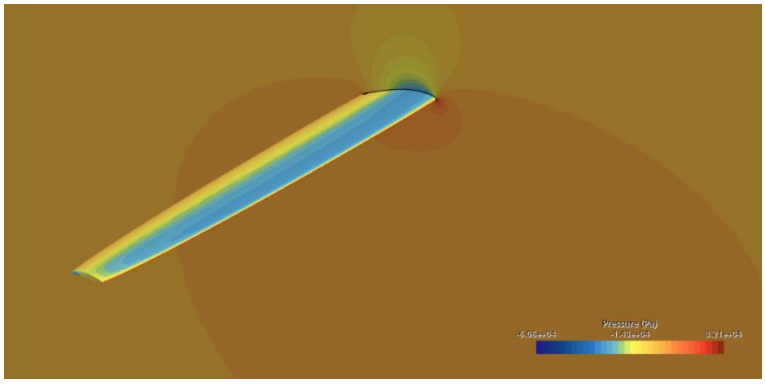

Figure 1-25: CFD analysis

The performance of the final design was validated by a similar CFD simulation. Following validation, the design was slightly swept backwards to ensure a more uniform flap length across the wingspan.

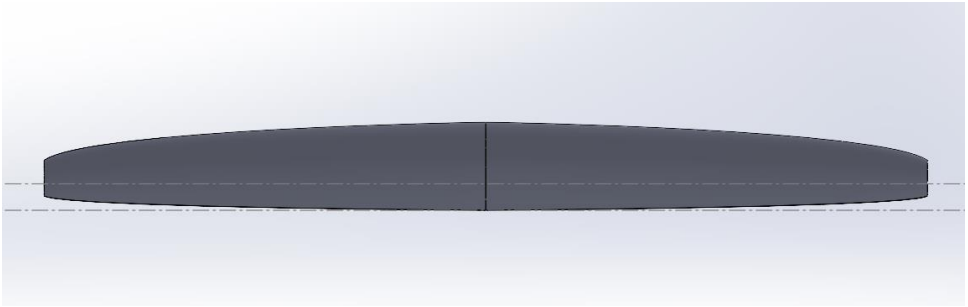

Figure 1-26: Main Foil

The same procedure was applied to the rudder, with an additional investigation into the possibility of incorporating an out-of-plane sweep. Comparison of various designs revealed that a moderate downward sweep resulted in efficiency improvements at different angles of attack at cruising speed. Consequently, the design that showed the greatest advantage was adopted.

Figure 1-27: Rudder foil

1.5.4 Structural analysis

Once the geometry and hydrodynamic characteristics of the foils and vertical appendages had been defined, the structural design began. The process follows a model-based approach, tailoring the modelling to the various analyses that need to be performed. The aim is to achieve the optimum balance between mechanical strength, performance and light weight.

After importing the geometries into *HyperMesh*, a mathematical model was generated to accurately represent the real connections, conditions, and loads associated with the designed T-foils' configuration.
The constraints of the model were carefully considered, in particular through the connection nodes representing the interface between the vertical appendages and the hull. The connection between the vertical appendage and the foil was treated using a non-linear contact formulation to ensure that the interface nodes moved together and transferred forces effectively. A comprehensive contact model was developed, tested and calibrated throughout the project.

A continuous interface and dialogue with the dynamic and overall design departments was maintained to identify the most critical working conditions from a structural point of view. The maximum hydrodynamic loads on the appendages during the service life were determined (listed in Table 1-4), with loads imported from previous CFD analyses. However, an appropriate safety factor (>2) was applied to account for dynamic effects.

	Centreboard take-off	**Centreboard Flight**	**Rudder**
Navigating speed	4 m/s	10 m/s	4 m/s
Incidence	0°	-2°	5°
Leeway angle	3°	3°	3°

Table 1-4: Operative conditions used for structural design

In terms of materials, we chose CFRP (Carbon Fiber Reinforced Polymer) for the unidirectional fibers, selecting high modulus fibers to mitigate the bending problems observed in previous years. In addition, glass and basalt fibers were selected to increase structural strength while minimizing the carbon footprint, and a filler foam with a density of 0.170 g/cm^3 was used to fill the cavities of the appendages.

Material	**Mechanical properties**	**Magnitude**
UD high modulus carbon fiber	E_1	390000 [MPa]
	E_2	12000 [MPa]
	v_{12}	0.322
TWILL carbon fiber	E_1	67298 [MPa]
	E_2	67298 [MPa]
	v_{12}	0.079
BIAX carbon fiber	E_1	15519 [MPa]
	E_2	15519 [MPa]
	v_{12}	0.173
BIAX basalt fiber	E_1	12252 [MPa]
	E_2	12252 [MPa]

	v_{12}	0.132
UD glass fiber	E_1	57200 [MPa]
	E_2	6531 [MPa]
	v_{12}	0.239

Table 1-5: Appendages materials

The analyses we carried out were:

- *Linear static analysis*: performed on the centerboard and rudder assemblies to study the maximum stresses and determine the appropriate lay-ups for component fabrication. In addition, a non-linear analysis was carried out to investigate the contact forces and conditions in the joint between the vertical appendages and the foils.
- *Linear buckling analysis*: carried out on the vertical centerboard and rudder. This was necessary due to the potentially dangerous compressive loads experienced by high aspect ratio components.
-

As a result of these analyses, the structure of the appendages was divided into main plies and smaller reinforcements to optimize material contribution. In addition to three full plies (a carbon twill, a +/- 45° basalt biaxial, and a UD glass ply), larger and smaller vertical reinforcements were incorporated, along with a small reinforcement for the link between the vertical and horizontal components.

Centerboard vertical	Centerboard foil	Rudder vertical	Rudder foil
Full	Full	Full	Full
Full	Full	Full	Full
Full	90° Large		Full
Large	Joint	Large	Large
Large	Full	Large	Large
Thin	Large	Thin	Thin
Thin	Thin	Large	90° centre
Joint	Joint	Thin	Joint
Full	Large		Joint
	Full		

TWILL carbon 200 g/m2	UD glass 160 g/m2
BIAX basalt 400 g/m2	UD carbon 400 g/m2
BIAX carbon 200 g/m2	

Table 1-6:T-foil stratifications (with legend on the side)

All analyses were carried out using the *Altair Optistruct* solver.

- *Static analysis*: results showed that the most stressed part are foils' fuselage sides and verticals' joints, primarily because of bending moment Contact forces and locations were within the expected ranges, demonstrating the anticipated behavior. Stress concentrations were observed, particularly in areas where there were variations in geometry and changes in the ply stack due to the presence of local reinforcements. Displacements showed a stiff behavior throughout the appendages, in line with the objective of achieving high stiffness for boat stability.

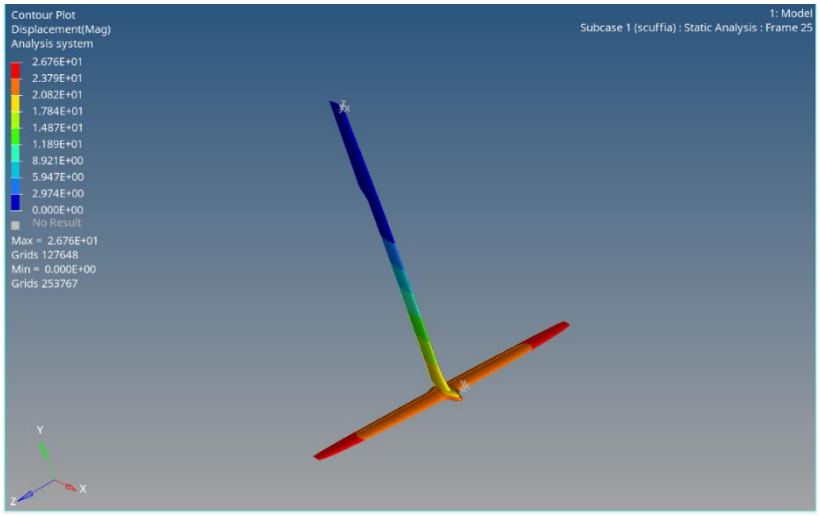

Figure 1-30: displacement on the centerboard

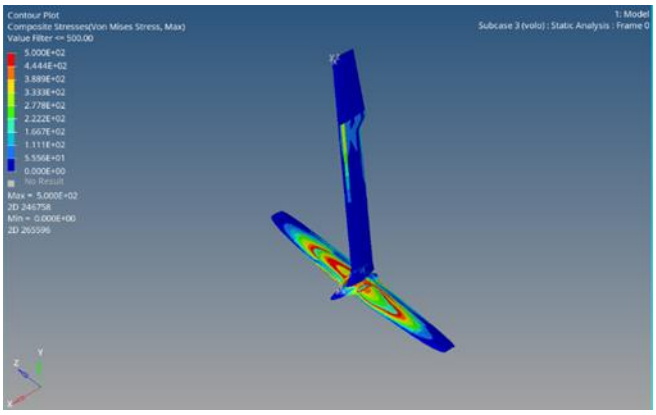

Figure 1-29: main foil stresses during flight

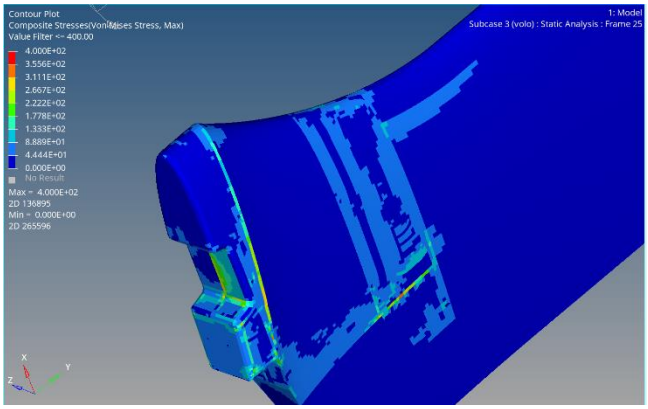

Figure 1-28: Stress on the vertical joint

It is worth remarking that the difference in the magnitude of the critical loads between the vertical centerboard and rudder is due to different boundary conditions.

According to the official rules of the Foiling SuMoth Challenge, a weight estimation was made to ensure that the percentage of CFRP used in the construction of the appendages was less than 50%.

1.6. Mechanical control system

The primary function of this system is to regulate the flight altitude of the moth, providing either lift or downforce by adjusting the angle of attack of its flap. Flight altitude is measured by the movement of the wand, which is linked to the horizontal transmission rod. The transmission rod is connected to the offset, enabling the adjustment of the flap's initial angle. This offset is then connected to an "L" shaped

mechanism, responsible for converting horizontal movement into vertical motion, ultimately leading to the adjustment of the vertical rod, which controls the flap.

Figure 1-31: VICTORIA's control system

VICTORIA has been carefully designed to be modular, allowing parts to be taken apart, replaced and interchanged with other boats. This year's development benefited from using SULA as a benchmark. This facilitated the redesign of inefficient systems and the improvement of those that were already satisfactory. Emphasis has been placed on improving the design to hide the systems as much as possible, resulting in a visually appealing and straightforward layout. The control system is designed to be dual, offering both mechanical and electronic options, with the flexibility for interchangeability between the two.

An initial proposal was to replace the Bugscam, used in SULA, with a continuous transmission system Although the Bugscam allowed changes in gradient over five zones, it proved inefficient due to difficulties in assembly and adjustment, resulting in either excessive interference and friction or excessive play. It was therefore proposed to install a support at the tip of the bowsprit, directly linking the wand to the transmission rod.

Two transmission alternatives were identified:

- Push rod: When the wand moves forward, the transmission rod pushes in the same direction, connecting to the offset, which then connects to the "L," exerting downward pressure on the flap adjustment rod.
- Pull rod: When the wand moves forward, the transmission rod pushes in the opposite direction, connecting to the lower end of an "I" structure, with a pin in its center, with the upper end connecting to the offset, achieving a change in direction. The offset then connects to the "L," pushing down the flap rod.

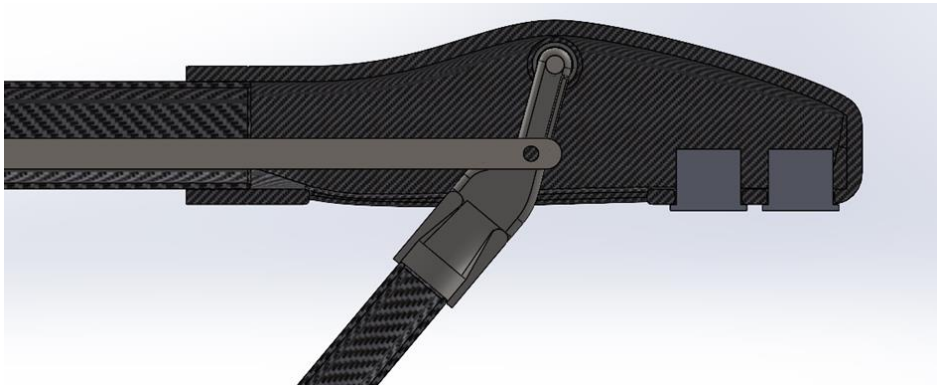

Figure 1-32: Control system section view

The pull rod provides a more flexible system with lower stresses, but carries the risk of delayed responses and reduced sensitivity.

The push rod was preferred as it provides direct transmission without changes in direction, minimizing clearance and interference, resulting in precise, reliable, and sensitive adjustments. However, the absence of constraints in the system leads to a stiffer setup, susceptible to greater stresses and deformations.

The “L” was designed to be able to connect with the offset and the electronic control system in 4 different places, allowing a sensitivity regulation.

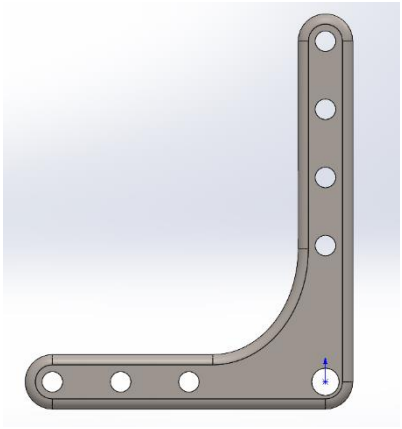

Figure 1-33: "L"

To ensure the wand's return, two alternatives are proposed:

- An axial spring connected to the transmission rod, providing the necessary push to rotate the wand.
- A torsion spring mounted directly on the fitting at the tip of the bowsprit, facilitating wand rotation, which then affects transmission height adjustments.

The axial spring was preferred because of its simplicity and ease of assembly and maintenance. For wand height adjustment, a telescopic system is considered, with the wand housed within a tube under tension from a spring. The sailor can pull the wand up using a rope passing inside the bowsprit.

1.7. Electronics and data acquisition

The project focuses on the design and integration of a wireless electronic control system to regulate the dynamics of small foiling boats. By seamlessly merging aerodynamics and hydrodynamics, our system is designed to enhance the performance, stability, and maneuverability of foiling boats, opening up new innovative frontiers for sailors.

1.7.1 Electronic Control System

Commercial Moth models rely on a set of different mechanical components to control the riding height of the boat. Although this has become the industry standard, this system can present several flaws.

The mechanical control system is cluttered and complex, since every aspect, from the riding height to the wand elastic tension, is adjusted with a sail rope. This adds up to the already complex sailing circuits of the moth. Other major issues include the mechanical slope which can lead to inaccurate and imprecise actuator responses on the push rod.

1.7.2 Introduction

To address the previously mentioned issues, the electronic control system has been designed with some guiding principles:

- Enhancing the overall **stability** and **maneuverability** of foiling boats, ensuring smooth transitions between foiling and non-foiling regimes.
- Developing a **user-friendly interface** for boat operators, allowing them to easily adapt, fine tune and monitor the foiling system, providing real-time feedback on the remote control.
- **Improving performances** by exploiting the possibility to set the foil at the minimum drag configuration, just before the take-off phase (ETO Enhanced Take Off).

Figure 1-34. First test on water

The electronic control system uses a servo motor to actuate the flap control surface of the main foil. A target ride height is initially selected by the sailor, who can adjust it later if needed. The system uses the feedback from the height sensor and from the

Inertial Measurement Unit (IMU) to feed the controller, which aims for the given target. The electronic controller surpasses the mechanical system in terms of performance by incorporating a GPS. This addition enables the system to improve the aerodynamic efficiency of the main foil, thereby enhancing its capabilities.

1.7.3 System Components

1.7.3.1 Ultrasonic Waterproof Sensor (JSN-srt04)

The ultrasonic sensor uses sonar impulses to determine the distance of an object, in this case, the height of the boat from the water surface. This module has a sensitive range of 20cm to 600cm with a tested measurement rate of 100 ~ 200ms. The sensor works by sending a high frequency sound through the ultrasonic transmitter, when signaled by the *trigger pin*. When the sound wave bounces off an object, it is reflected back to the module. The sensor then "listens" for the ultrasonic sound with the ultrasonic receiver and then sends data via the *echo pin*. As the speed of sound in air is known and the sensor records the time between *trig and echo,* it is possible to calculate the distance to the object.

1.7.3.2 Servo Motor Hitec D845WP IP67

A servo motor is a rotary actuator that allows for precise control of angular position, velocity and acceleration in a mechanical system[2]. It is coupled with a sensor for position feedback, enabling accurate control of its motion and final position. The chosen motor model is selected for its capabilities in providing the required strength, speed, and precision for the application.

Voltage [V]	Torque [kg/cm]	Speed [Sec/60grd]
4.8	32,5	0.26
6.0	40,5	0.21
7.4	50,0	0.17

Table 1-7

The servo motor is the only moving element of the system, through a single lever the servo-arm is connected to the flap rod, and this allows the motor to operate directly on the flap's angle on the main foil.

1.7.3.3 Esp32 D1 Mini

ESP32 is a series of low-cost, low-power system on a chip microcontroller with integrated Wi-Fi and dual-mode Bluetooth. The mini version is ideal for our needs: offering the same performance as the standard size but in a more compact form

[2] Wikipedia

with fewer GPIO pins. This model is crucial for processing the data from the ultrasonic sensor.

1.7.3.4 Battery Shield V1.2.0 for D1 Mini

This battery shield powers the ESP32 D1 mini with a mobile power supply, supporting quick charging times with a maximum current of 1000 mA. It includes an integrated charge controller with automatic shut-off, ensuring the battery is protected against overcharging.

1.7.3.5 ElioIOT

ElioIOT is a complete development board with a variety of built-in sensors and functionalities, including Light Sensor, Pressure and Altitude, Laser Distance, Accelerometer and Gyro, MicroSD Slot, charging support. The board is powered by a more powerful version of the Esp32 series, the Esp32-S3. This module also includes several GPIO pins, allowing it to effectively control various components.

Figure 1-35:ElioIOT

1.7.3.6 Neo-6m GPS module

The NEO-6M GPS module is a high-performance, all-in-one GPS receiver with a built-in, powerful satellite search function. Power and signal indicators allow the module's status to be monitored. The data backup battery allows the module to save the data in case the main power supply is accidentally switched off.

1.7.3.7 LCD Module 2004 20x4 i2c interface

This LCD module provides users with useful information and allows system settings to be modified, fine-tuned and parameters to be visualized.

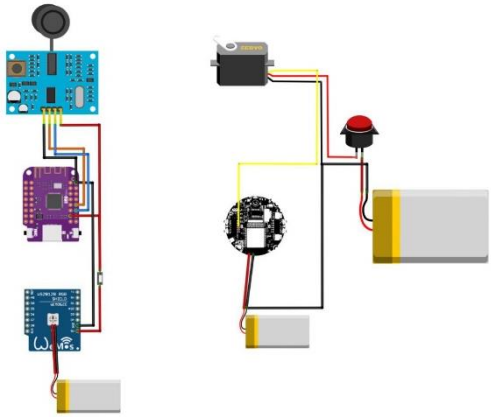

Figure 1-36: Circuit diagram

1.7.3.8 Additional Components

1.7.3.8.1 3D printer

The system relies on 3D printing for the encapsulation of all the sensors, the housings are printed with PLA and the openings are waterproofed with a silica ring and a set of screws. The servo motor case is also 3D printed, providing protection and an easy mounting point on the boat.

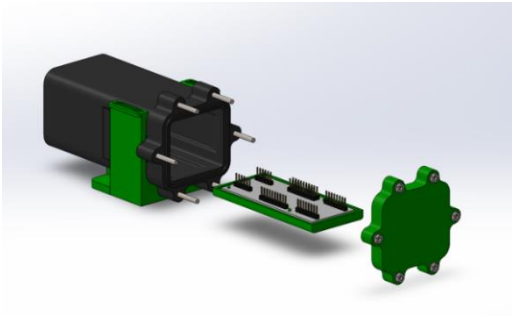

Figure 1-37: 3D printed waterproof box

1.7.3.8.2 Batteries

All the microcontrollers are powered by a LiPo rechargeable battery 3.7 V 2000mAh 1S. The servo motor is instead powered with a LiPo rechargeable battery 7.4 V 4500mAh 2S 25c.

1.7.3.8.3 Waterproof On/Off Switch

A waterproof self-lock switch is added to power off and power on the servo motor only when needed.

1.7.4 System Composition Overview

The control system is based on a two-tier architecture, consisting of a central hub and several independent sensor nodes. The aim is to improve the system's resilience to the harsh operating environment. By making each module independent, it is possible to avoid at least one potential single point of failure, making the system more secure. Communication between the nodes is based on WIFI IEEE 802.11. A specially designed packet system is used. This means less cabling on both the boat and the modules, making maintenance easier and quicker.

1.7.4.1 Distance nodes

Each sensor node is equipped with an ESP32 Mini D1, a LiPo battery, a battery shield, and a JSN-srt04, it operates as a self-contained unit, encapsulated in a waterproof box, responsible for calculating the height. To improve the reliability of the system, two of these modules co-exist for redundancy: one is always active, the other is on standby waiting for an error to happen. As soon as the first module stops working properly, the hub signals to the backup one to start sampling.

1.7.4.2 Distance nodes position

Since the modules' ultrasonic transmitter and ultrasonic receiver need to be exposed to measure the distance, the ideal position is under the bowsprit head. Cables are routed through the bowsprit up to the deckhouse where they meet the actual sensor nodes.

Figure 1-38: Ultrasonic sensor (in gray) under the bowsprit head

1.7.4.3 Hub

The central hub is equipped with an ElioIOT module, a LiPo battery and the neo-6m gps module. It plays a central role in collecting, processing and storing data from the distributed sensor nodes. The hub takes advantage of the dual-core CPU architecture of the Esp32-s3 provided by the ElioIOT board, with one core dedicated to handling all the communications coming from the range modules, the GPS module and the remote control, while the other core is dedicated to the control task. This allows the hub to perform both tasks with maximum efficiency, reducing latency. The hub's waterproof box also houses the battery that powers the servo motor.

1.7.4.4 Hub Position

The designated hub position is inside the deckhouse, which is optimal for both component safety and access time. A cable runs from the hub to the servomotor, which is conveniently located near the hand crank that controls the hatch.

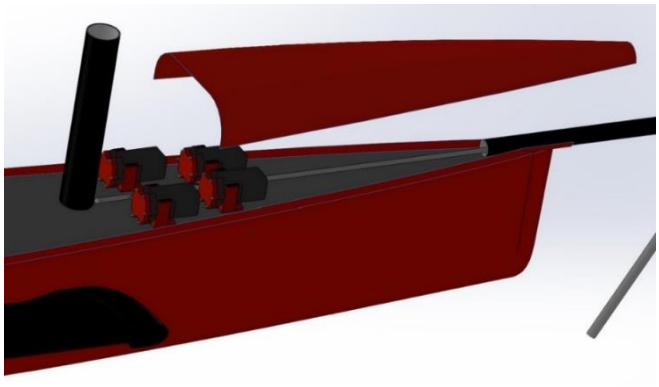

Figure 1-39:Box position

1.7.5 Flight Control

The flight control flow starts at the distance node where the water distance is calculated every 100 ~ 200ms, this bottleneck depends only on the ultrasonic sensor type. After the calculation, the data is sent to the hub where some pre-processing takes place, outliers are removed with a median filter, this ensures more safety if the received distance is not in the expected range, also a correction on the measured height is performed by applying trigonometric to take into account the roll and pitch conditions. The angle of the corrections is obtained from ElioIOT's built-in IMU, so that a more accurate distance value is used in the control operations.
Flight control relies on the Proportional–Integral–Derivative controller (PID), which is suitable because the dynamic modelling of the boat-sailing system is extremely non-linear and can be a trivial task.

1.7.6 PID controller

A proportional-integral-derivative (PID) controller is a control loop mechanism that uses feedback. A PID controller continuously calculates the error between a target point (r(t) - target height) and a measured variable (y(t) - actual height) and applies corrections based on three parameters: Proportional (Kp), Integral (Ki), Derivative (Kd).
The controller tries to minimize the error by constantly adjusting the manipulated variable. These adjustments are calculated as a weighted sum of the control terms.

$$wd_c = K_P * e(t) + K_I \int e(t) + K_D \frac{de(t)}{dt}$$

$$\mathrm{e(t)} = \mathrm{r(t)} - \mathrm{y(t)}$$

Equation 1-2: PID Equation

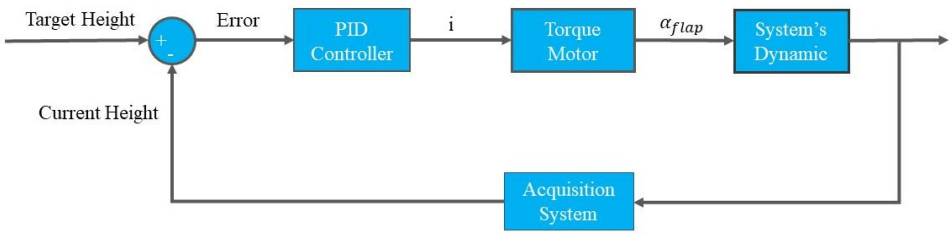

Figure 1-40: Eletronic System Control Model

1.7.7 Parameters tuning

Each of the tree PID parameters gives a different behavior:

- The *Kp* term determines how proportional the control output should be to the error. If only the proportional term is used, there will be an error between the setpoint and the process value, as the proportionality depends on the error itself.
- The *Ki* term takes into account the past values, it tries to eliminate the residual error by adding a control action due to the historic cumulative value of the error. As the error disappears, the integral also stops growing, reducing the effect of the proportional as the error decreases.
- The *Kd* term is the estimate for the future term, it tries to reduce the future error based on the current error rate trend, so larger changes produce larger control effects.

Based on the previous assumptions we investigated the case of a PI controller by setting Kp = 0.8, Ki = 0.5 and Kd = 0.0. The decision to set the derivative to zero is determined by the fact that a derivative action on the controller could affect the overall stability of the flight, without appropriate filtering.

1.7.8 Adaptive Parameters

The output of the system is the flap angle calculated by the controller to achieve and maintain the selected altitude. To further improve the performance of the controller, an adaptive parameter technique is used. This trick allows the system to autonomously change the configuration of the PI, thus changing its behavior. The initial parameters are set as described in the previous paragraph, then as the boat approaches the target height, these coefficients are slowly modified until saturation is reached, in order to obtain a more conservative configuration that can maintain the target altitude more smoothly improving stability.

1.7.9 Enhanced Take Off (ETO)

One of the main purposes of the electronic system is to improve the performance of the mechanical system, and this has led to the development of a new way of taking off. The boat is designed to start the flight at a certain speed and in order to make it easier to reach the foiling speed, this new feature ties the main foil flap in a neutral position where it produces the least amount of drag. This allows the boat to start foiling before the conventional speed improving its efficiency.

1.8. Gantry

1.8.1 Design

The gantry is the structure that holds the rudder in place. For aerodynamic and aesthetic reasons, we decided to use a closed shell structure rather than the usual tubular structure. After a careful selection of the design, we went on to trace the construction lines of the geometry and define this shape:
As we have several regulatory constraints, we need a solid geometry that integrates the tubular structure, which has the task of absorbing all the loads that come from the vertical of the rudder. We then looked at the range of action and the most appropriate way of attaching it to the transom, while remaining within the constraints.

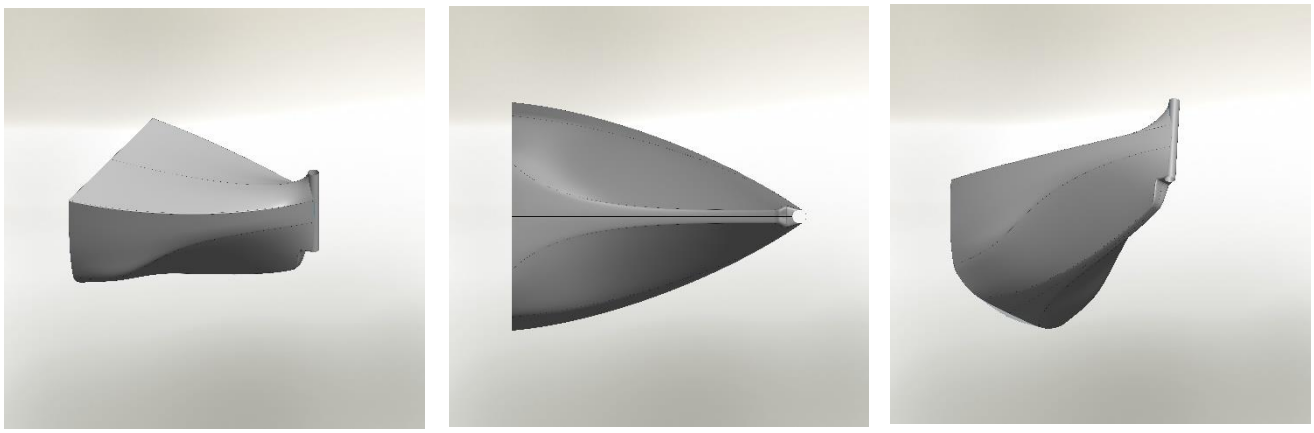

Figure 1-41: Gantry desing

1.8.2 Stratification and analysis procedure

Once we'd designed the shape of the component, our structural division worked on the layering. Since the part must be fixed to the transom of the boat and support the rudder fitting in position, it is subject to certain loads. A dynamic analysis of the boat allowed us to define the loads at the level of the rudder. These loads allowed us to define the most stressed planes, areas and directions.

The load definition highlighted critical areas of the component that were subject to traction and others that were subject to compression. The lower part is mainly subjected to tension, while the upper part is subjected to compression when the mold is closed. As the stiffness of the component is proportional to the stiffness of the boat during sailing, the component must ensure low deformation and high stiffness values. The compact shape of the part should allow the moment of inertia to provide a satisfactory level of stability and stiffness, allowing the first layering decisions to be made. We decided to divide the component into three different lay-ups according to the loads applied and the geometry.

The following table provides an overview of the chosen materials and their primary and secondary Young's modulus as well as thicknesses used in the analysis above.

Materials	LAP	Thickness	E1	E2
MINERAL FIBRE – TWILL 220	10+5mm	0.15mm	31449Mpa	31449Mpa
MINERAL FIBRE – UD 300	10+5mm	0.25mm	36115Mpa	8712Mpa
MINERAL FIBRE –BIAX 450	10+5mm	0.40mm	15000Mpa	15000Mpa
CARBON FIBRE – UD 400	10+5mm	0.39mm	163488Mpa	8193Mpa
CARBON FIBRE – BIAX 200	10+5mm	0.20mm	15000Mpa	15000Mpa
CQI TUBE Ø20 sp.2mm		2.00mm	150000Mpa	150000Mpa
PET 6mm		6.00mm	112Mpa	isotropic
OKUME' 6mm		6.00mm	7900Mpa	isotropic

Table 1-8: Table of materials

Following this, an FEM analysis was conducted on the piece to gain preliminary insight into the stratification ideas that had been decided upon. Prior to commencing this analysis, it was necessary to mesh the shell surface. In this case, as the loads were applied to the tube, which is laminated between the inner skin and outer skin layers, the meshing process involved a fast 3D procedure. The external surface had been offset inwards, to apply the loads on the tube's external surface. The point of application of the force had been defined as a rigid independent point, with multiple dependent points on the top and bottom tube's edges. Then we defined the constraints acting on the vertical surface, facing the transom.

Figure 1-42: masterplates

Three masterplates are employed to constrain the gantry at the transom. These mechanical joints are easy to install as they will be glued to the lamina, they are lightweight, and exhibit good mechanical properties. For our purpose, we opted for a M8 thread solution. The bending stresses acting on the piece, create a traction and contraction dynamic load condition which guided our decision.

The three glued masterplates act on specific regions of the gantry surface, opposite to the transom, where Okumé rectangular panels are laminated as the core. This choice allowed us to define the constraint given by the masterplates as if a node were acting uniformly over the entire surface of interest. As the panel is threatened and glued to it, the loads will be uniformly distributed.

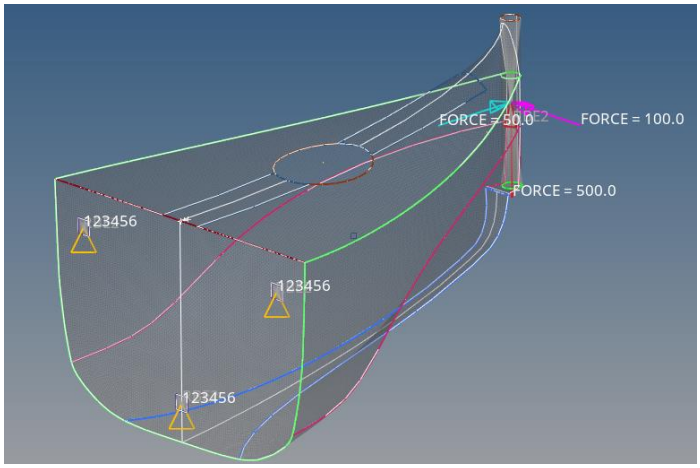

Figure 1-43: Detail of materials with loads and constraints

Once the constraints and the loads were defined, the workflow could proceed by highlighting the areas of the reinforcement's positions:

- Unidirectional reinforcement on the top part of the gantry
- Unidirectional reinforcement on the bottom part of the gantry
- PET reinforcement on the bottom part of the gantry

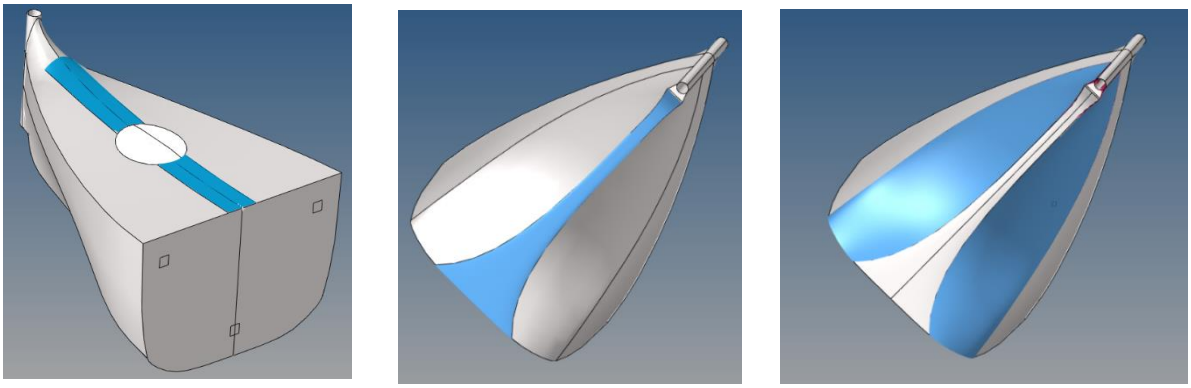

Figure 1-44: UD reinf. top, UD reinf- bottom, PET reinf. Bottom (from left to right)

The analysis was carried out under two main working conditions, defining the two possible transverse sailing directions. The analysis showed some clear results in terms of the stresses experienced and the maximum deflection. More precisely, the maximum deflection has a value of 9 mm, with dangerous working conditions (20 knots). On the other hand, the Von Mises stresses on the surfaces are shown in the following FEM analysis.

Thanks to this analysis, we were able to reduce the weight of the component by 0.7kg, compared to the first preliminary lay-up. The theoretical weight of the part is 1.5kg. We could not remove any more material because of the stiffness target.

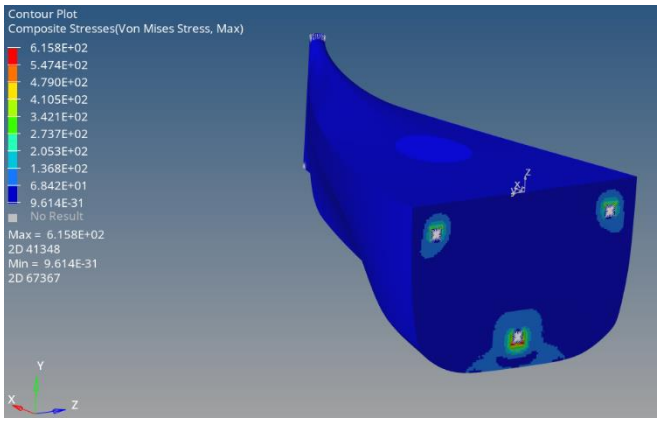

Figure 1-45: Von Mises Stresses acting on the component

1.9. Rig

As for the choice of rig, we started by deciding on the type of sail we wanted to use and ended up with a decksweeper. The other components were then selected accordingly. This type of sail offers greater aerodynamic efficiency compared to a traditional sail due to the endplate effect, and its lowered center of sail makes the boat easier to handle in stronger wind conditions. To minimize cost and waste, we opted for a used 2019 Lennon sail. The choice of decksweeper also influenced the design of the boat, as we needed to project a deckhouse to provide a seal between the sail and the boat to maximize its benefits..

A re-use philosophy was also adopted for the boom and mast, with the choice of a second-hand Z boom and CST Tow Pro mast.

In order to optimize the layout of the deck circuits, the organizers were designed with a 3D printed base and two basalt fiber and bio-resin laminated panels to provide the best compromise between sustainability and mechanical properties. A basalt fiber plate was also made to house the cleats and pulleys. Both the organizers and the plate have been designed with a 15-degree angle to the horizontal to make them easier to use and to guide the ropes to the wings.

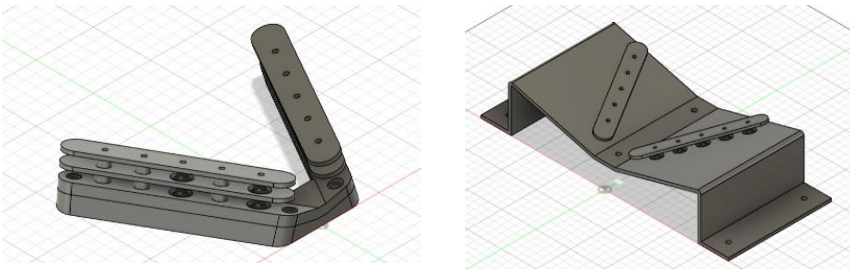

Figure 1-46. organizers

2. MANUFACTURING AND COST ANALYSIS

2.1. Manufacturing choices

This section provides a theoretical overview of the production processes chosen for the realization of VICTORIA. Detailed descriptions of the actual production will be covered in detail in report S2.

Following the engineering discussion on material selection in the first part of this report, and the forthcoming sustainability analysis in the next section, our aim is now to define and justify specific production decisions. These decisions, some of which have already been put into practice while others will be finalized in the coming days are critical to ensure that we succeed in completing the manufacturing phase.

2.2. Hull

For the construction of the hull mold, we have decided to use the Strip Planking technique, based on the methods and cost analyses from previous years. This technique involves placing thin, highly elastic wooden strips side by side on ribs that form a skeletal framework. This approach allows us to achieve the desired curvature of the hull. We already employed this construction method in the past to create a plug, which was then used to produce the actual fiber mold for KETH; however, this time we will directly create the female mold. This adjustment will reduce both production time and material waste, as the plug used for mold construction will no longer be necessary.
To ensure precision, the frames will be placed with equidistant and parallel spacers of uniform length. Lime-wood strips will then be laid on top, secured with nails during assembly, and glued together with vinyl glue.
For the bow section of the mold, we decided to use a milled PU foam block. This decision was made due to the difficulty of placing the slats in such a small area while maintaining perfect geometry. After assembling the foam

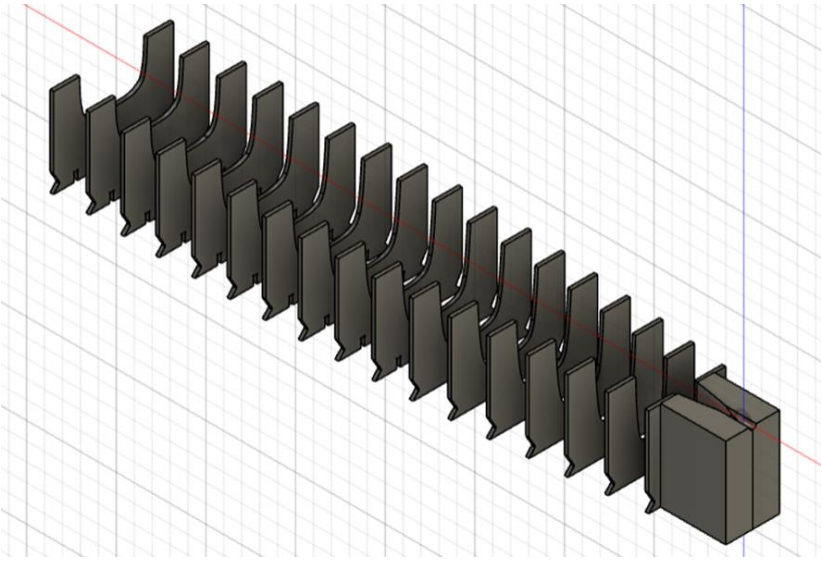

Figure 2-1: hull mold

block, we will sand and grout the surface to ensure a homogeneous finish. To ensure impermeability, the inside of the mold will be reinforced with glass fiber twill and coated with resin before being painted to cover any microporosity.

The second innovation in our production process involves the lamination technique. Unlike the manual lamination used for KETH and SULA, this year we are adopting the Infusion technique. Experimental data indicate that this method produces less void content within the lamination and uses less resin, improving the strength and quality of the final product.

2.3. Deck

As mentioned in the previous section, part of VICTORIA's deck will be repurposed from team scrap that was deemed unusable due to dimensional issues. This material will be used to make the panel that covers the circuits and housing for the wings, as well as the flat bow section of the deck.

The mold for the new part of the deck is made from wood, which is milled and then coated with resin to make it waterproof. To minimize waste and reduce the number of wooden panels required, the mold will be divided into several parts and assembled using centering pins. The production of the deck will follow the same procedure as that of the hull.

2.4. Wings, Gantry and Appendages

For the wings and the gantry, we have decided to use lamination for the first time. Both components will be produced using female wooden molds, which will be used for manual lamination. Due to its size, the gantry mold will be made in several parts that will be assembled after milling.

Regarding the appendages, we will use Rakutool for the molds. This material is well-suited to the machining process and ensures a high-quality final product. The production process will follow the same methods used for SULA.

3. SUSTAINABILITY ANALYSIS

3.1. General description

The idea behind this project is to create a boat that will last over time. To achieve this goal, while leaving room for improvement and development for both the boat and the team, it was decided to focus more on the hull to make it functional, sustainable, and durable. Sustainability has been extended to all the other components by trying to reuse different types of waste obtained from some companies. Another aspect working in our favor is the fact that we are a student team with a solid and somewhat experienced background; this has allowed us to fill our warehouse with scraps from less successful work and with broken or disused components from old boats, which we have tried to reuse wherever was possible for the VICTORIA project.

3.2. Boat and elements lifecycle

3.2.1 Hull

The hull mold is made of poplar and lime wood. Wood is an easily obtainable material, with a low carbon footprint, and its industrial processing requires limited use of fossil fuels and reduced consumption of resources (such as water) compared to other materials. It was decided to opt for a female mold to avoid having to make a plug as well. PET from industrial waste, plastic bottles and caps was chosen for the core, with the possibility of melting and recycling the various pieces in the future to obtain sheets of different sizes for other uses. The fiber used is basalt, which has a lower environmental impact compared to, for example, fiberglass.

3.2.2 Deck

The initial idea was to reuse an old deck from the warehouse, which had not been used for any boat due to imperfections. However, using this panel entirely would have required extensive modifications to accommodate the wings and all the inserts, leading to increased production of fiber and resin waste from various processes. Therefore, it was decided to use the old deck only for the bow section and to create a male mold made of multilayered poplar wood for the stern section, where all the fittings are required.

3.2.2 Other elements

The goal is to build a boat using almost exclusively basalt fiber. The gantry has been entirely designed using basalt, while the foils will be crafted from a combination of

carbon and basalt fibers. This approach reduces the maximum carbon percentage allowed by regulations by approximately 10%. For the rig, we chose to use a second-hand to avoid higher costs and lower our environmental impact.

3.3. Action for a sustainable future

In the context of sustainability within the maritime sector, there is a deep reflection on responsibility towards the marine environment and future generations. Indeed, it is widely acknowledged that the maritime industry has a significant impact on the marine ecosystem and it is therefore vital to find sustainable solutions to mitigate it.

In terms of potential solutions, bio-based composites emerge as one of the most promising options. Derived from renewable resources such as plants or recycled biomass, these materials offer numerous environmental advantages over conventional counterparts. Firstly, they have a lower ecological footprint as they reduce dependence on fossil resources and limit greenhouse gas emissions during production. This is particularly relevant in the maritime industry where the production of ships can involve high energy consumption and emissions of pollutants. Secondly, they can help address the issue of marine litter, as many of them are biodegradable or recyclable at the end of the boat's lifecycle. This is a critical advantage, considering the prevalent issue of plastic and synthetic materials polluting our oceans.
However, it is important to acknowledge that bio-based composites are not a universal solution and there are challenges to be addressed. For example, the availability of sufficient plant biomass to meet the demand of the maritime industry may be limited, potentially leading to competition with food production. Therefore, it is essential to conduct further research and develop effective strategies to overcome these challenges.
Bio-based composites thus represent one of the most promising options for promoting sustainability in the maritime industry, but a holistic approach is necessary, including improvements in production processes, eco-friendly design, and targeted policies/regulations. Indeed, efficient boat design helps to lower water resistance and improve aerodynamics to reduce fuel consumption and pollutant emissions; while, from the perspective of governmental policies and regulations, fiscal incentives could be introduced for the use of clean technologies, stricter regulations on the use of harmful materials, and certification programs to promote environmental sustainability in the sector.
On our part, as a student team, we focus heavily on the design aspect by adopting more hydrodynamic hull shapes, optimizing and balancing boat weight, using lightweight materials, and minimizing superstructure to improve efficiency. Additionally, we are exploring potential bio-based alternatives to the materials we currently use that can align with our means and economic capabilities.

4. TEAM

- Professor (Team Manager): Giuliana Mattiazzo
- Team leader (Logistic Officer): Maurizio De Franchi
- Product Manager (Team Captain): Leonardo Romano
- Project Manager (Team Co-Captain – Communication officer): Aurora Caloni
- Fluid-dynamics: Dario Vucinic, David Victor Azzaro Bradea, Martino Fabbro, Filippo Avidano, Elia Indelicato, Maksym Malyshev
- Structure: Francesco Fogliati, Simone Pintaldi, Rabbi Golam, Lorenzo Valle, Alessandro Galasso, Luca Corucci
- Sustainability: Francesca Scarascia
- Electronics: Andrea Sillano, Lorenzo Barbati, Andrea Di Nezza, Giorgia Giacalone
- Mechanical control System: Bernardo Fagundes
- CNC mill: Marco Balestreri
- Manufacturing: Samuele Mastrobisi, Riccardo Pappalardo, Arianna Bonino, Matilde Giuliano, Elisa Tomasi, Lorenzo Pistolesi, Luca Pastorelli, Carlotta Maria Marro
- Sailors: Deniz Ali Yenigun, Giuseppe Piccirilli, Oytun Erdogan
- Communication: Mattia Santarosa, Giulio Ranocchia

5. BIBLIOGRAPHY

Abt, C., S.D. Bade, L. Birk, e S. Harries. «Parametric Hull Form Design — A Step Towards One Week Ship Design». In *Practical Design of Ships and Other Floating Structures*, 67–74. Elsevier, 2001. https://doi.org/10.1016/B978-008043950-1/50009-0.

Armanfar, Arash, A. Alper Tasmektepligil, Recep Tayyip Kilic, Serdar Demir, Serhat Cam, Youness Karafi, Badr Abou El Majd, e Erkan Gunpinar. «Embedding Lattice Structures into Ship Hulls for Structural Optimization and Additive Manufacturing». *Ocean Engineering* 301 (giugno 2024): 117601. https://doi.org/10.1016/j.oceaneng.2024.117601.

Bagheri, Hassan, e Hassan Ghassemi. «Optimization of Wigley Hull Form in Order to Ensure the Objective Functions of the Seakeeping Performance». *Journal of Marine Science and Application* 13, fasc. 4 (dicembre 2014): 422–29. https://doi.org/10.1007/s11804-014-1275-5.

Biliotti, Iacopo, Stefano Brizzolara, Michele Viviani, Giuliano Vernengo, Danilo Ruscelli, Domenico Guadalupi, e Andrea Manfredini. «Automatic Parametric Hull Form Optimization of Fast Naval Vessels», 2011.

Bole, Marcus. «Parametric Generation of Yacht Hulls», 1997.

Cavazzuti, M., e M. A. Corticelli. «Optimization of Heat Exchanger Enhanced Surfaces through Multiobjective Genetic Algorithms». *Numerical Heat Transfer, Part A: Applications* 54, fasc. 6 (27 agosto 2008): 603–24. https://doi.org/10.1080/10407780802289335.

Chang, Haichao. «Sampling Method for Hull Form Optimization Based on the Morphing Method and Its Application». *Ocean Engineering*, 2023.

Erdem, Ceyhan, Yoann Eulalie, Philippe Gilotte, Stefan Harries, e Christian N. Nayeri. «Aerodynamic Optimization of a Reduced Scale Model of a Ground Vehicle with a Shape Morphing Technique». *Fluids* 7, fasc. 5 (10 maggio 2022): 166. https://doi.org/10.3390/fluids7050166.

Gao, Ting, Yaxing Wang, Yongjie Pang, e Jian Cao. «Hull Shape Optimization for Autonomous Underwater Vehicles Using CFD». *Engineering Applications of Computational Fluid Mechanics* 10, fasc. 1 (gennaio 2016): 599–607. https://doi.org/10.1080/19942060.2016.1224735.

Gaspar-Cunha, Antonio, e Armando Vieira. «A Hybrid Multi-Objective Evolutionary Algorithm Using an Inverse Neural Network», s.d.

Gerhardt, Frederik C. «Unsteady Aerodynamics of Upwind-Sailing and Tacking», s.d.

Hamed, Ahmed. «Multi-Objective Optimization Method of Trimaran Hull Form for Resistance Reduction and Propeller Intake Flow Improvement». *Ocean Engineering* 244 (gennaio 2022): 110352. https://doi.org/10.1016/j.oceaneng.2021.110352.

Han, Soonhung, Yeon-Seung Lee, e Young Bok Choi. «Hydrodynamic Hull Form Optimization Using Parametric Models». *Journal of Marine Science and Technology* 17, fasc. 1 (marzo 2012): 1–17. https://doi.org/10.1007/s00773-011-0148-8.

Harries, S., e C. Abt. «Faster Turn-around Times for the Design and Optimization of Functional Surfaces». *Ocean Engineering* 193 (dicembre 2019): 106470. https://doi.org/10.1016/j.oceaneng.2019.106470.

Harries, Stefan, e Sebastian Uharek. «Application of Radial Basis Functions for Partially-Parametric Modeling and Principal Component Analysis for Faster Hydrodynamic Optimization of a Catamaran». *Journal of Marine Science and Engineering* 9, fasc. 10 (29 settembre 2021): 1069. https://doi.org/10.3390/jmse9101069.

Izaguirre Alza, Patricia. «Numerical and Experimental Studies of Sail Aerodynamics». PhD Thesis, Universidad Politécnica de Madrid, 2012. https://doi.org/10.20868/UPM.thesis.14885.

Keser, Robert. «Parametric Aft Hull Optimisation of Semi- Displacement Vessel Using CFD», s.d.

Khan, Shahroz, Erkan Gunpinar, e Kemal Mert Dogan. «A Novel Design Framework for Generation and Parametric Modification of Yacht Hull Surfaces». *Ocean Engineering* 136 (maggio 2017): 243–59. https://doi.org/10.1016/j.oceaneng.2017.03.013.

Khan, Shahroz, Erkan Gunpinar, e Bekir Sener. «GenYacht: An Interactive Generative Design System for Computer-Aided Yacht Hull Design». *Ocean Engineering* 191 (novembre 2019): 106462. https://doi.org/10.1016/j.oceaneng.2019.106462.

Kostas, K.V., A. Amiralin, S. Sagimbayev, T. Massalov, Y. Kalel, e C.G. Politis. «Parametric Model for the Reconstruction and Representation of Hydrofoils and Airfoils». *Ocean Engineering* 199 (marzo 2020): 107020. https://doi.org/10.1016/j.oceaneng.2020.107020.

Kramer, Mara E. «Automating Lackenby's Method: The Design of a Set of Scripts to Execute Lackenby's Method with McNaull's Expansion in Rhinoceros 3D», s.d.

Li, Anlun. «CFD Optimization of Hydrofoiling Concept for A New Era of Sea Transports», s.d.

Liu, Xinwang, Weiwen Zhao, e Decheng Wan. «Multi-Fidelity Co-Kriging Surrogate Model for Ship Hull Form Optimization». *Ocean Engineering* 243 (gennaio 2022): 110239. https://doi.org/10.1016/j.oceaneng.2021.110239.

Lujan-Moreno, Gustavo A., Phillip R. Howard, Omar G. Rojas, e Douglas C. Montgomery. «Design of Experiments and Response Surface Methodology to Tune Machine Learning Hyperparameters, with a Random Forest Case-Study». *Expert Systems with Applications* 109 (novembre 2018): 195–205. https://doi.org/10.1016/j.eswa.2018.05.024.

Marrone, S., B. Bouscasse, A. Colagrossi, e M. Antuono. «Study of Ship Wave Breaking Patterns Using 3D Parallel SPH Simulations». *Computers & Fluids* 69 (ottobre 2012): 54–66. https://doi.org/10.1016/j.compfluid.2012.08.008.

Mason, Andrew Phillip. «STOCHASTIC OPTIMISATION OF AMERICA'S CUP CLASS YACHTS», s.d.

Matsui, Sadaoki. «A New Mathematical Hull-Form with 10-Shape Parameters for Evaluation of Ship Response in Waves». *Journal of Marine Science and*

Technology 27, fasc. 1 (marzo 2022): 508–21. https://doi.org/10.1007/s00773-021-00849-3.

Mohammed Sahib, Mortda, e György Kovács. «Multi-Objective Optimization of Composite Sandwich Structures Using Artificial Neural Networks and Genetic Algorithm». *Results in Engineering* 21 (marzo 2024): 101937. https://doi.org/10.1016/j.rineng.2024.101937.

Percival, Scott, Dane Hendrix, e Francis Noblesse. «Hydrodynamic Optimization of Ship Hull Forms». *Applied Ocean Research* 23, fasc. 6 (dicembre 2001): 337–55. https://doi.org/10.1016/S0141-1187(02)00002-0.

Priftis, Alexandros, Evangelos Boulougouris, Osman Turan, e Georgios Atzampos. «Multi-Objective Robust Early Stage Ship Design Optimisation under Uncertainty Utilising Surrogate Models». *Ocean Engineering* 197 (febbraio 2020): 106850. https://doi.org/10.1016/j.oceaneng.2019.106850.

Sanches, Filipa. «Parametric Modelling of Hull Form for Ship Optimization», s.d.

Spinosa, Emanuele, Riccardo Pellegrini, Antonio Posa, Riccardo Broglia, Mario De Biase, e Andrea Serani. «Simulation-Driven Design Optimization of a Destroyer-Type Vessel via Multi-Fidelity Supervised Active Learning». *Journal of Marine Science and Engineering* 11, fasc. 12 (25 novembre 2023): 2232. https://doi.org/10.3390/jmse11122232.

Stephens, D W, e P D Fawell. «OPTIMISATION OF PROCESS EQUIPMENT USING GLOBAL SURROGATE MODELS», 2012.

Vasudev, K. L., R. Sharma, e S. K. Bhattacharyya. «Multi-Objective Shape Optimization of Submarine Hull Using Genetic Algorithm Integrated with Computational Fluid Dynamics». *Proceedings of the Institution of Mechanical Engineers, Part M: Journal of Engineering for the Maritime Environment* 233, fasc. 1 (febbraio 2019): 55–66. https://doi.org/10.1177/1475090217714649.

Winter, Roy de, Bas van Stein, Thomas Bäck, e Thijs Muller. «Ship Design Performance and Cost Optimization with Machine Learning», s.d.

Zakerdoost, Hassan, e Hassan Ghassemi. «Probabilistic Surrogate-Based Optimization of Ship Hull-Propulsor Design with Bi-Level Infill Sampling Technique». *Ocean Engineering* 286 (ottobre 2023): 115614. https://doi.org/10.1016/j.oceaneng.2023.115614.

Zhang, Ping, De-xiang Zhu, e Wen-hao Leng. «Parametric Approach to Design of Hull Forms». *Journal of Hydrodynamics* 20, fasc. 6 (dicembre 2008): 804–10. https://doi.org/10.1016/S1001-6058(09)60019-6.

Zhou, Hui, Baiwei Feng, Zuyuan Liu, Haichao Chang, e Xide Cheng. «NURBS-Based Parametric Design for Ship Hull Form». *Journal of Marine Science and Engineering* 10, fasc. 5 (18 maggio 2022): 686. https://doi.org/10.3390/jmse10050686.

———. «NURBS-Based Parametric Design for Ship Hull Form». *Journal of Marine Science and Engineering* 10, fasc. 5 (18 maggio 2022): 686. https://doi.org/10.3390/jmse10050686.